An evolving view on biogeochemical cycling of iron

Andreas Kappler[1,4]✉, *Casey Bryce*[2,4], *Muammar Mansor*[1], *Ulf Lueder*[1], *James M. Byrne*[2] *and Elizabeth D. Swanner*[3]

Abstract | Biogeochemical cycling of iron is crucial to many environmental processes, such as ocean productivity, carbon storage, greenhouse gas emissions and the fate of nutrients, toxic metals and metalloids. Knowledge of the underlying processes involved in iron cycling has accelerated in recent years along with appreciation of the complex network of biotic and abiotic reactions dictating the speciation, mobility and reactivity of iron in the environment. Recent studies have provided insights into novel processes in the biogeochemical iron cycle such as microbial ammonium oxidation and methane oxidation coupled to Fe(III) reduction. They have also revealed that processes in the biogeochemical iron cycle spatially overlap and may compete with each other, and that oxidation and reduction of iron occur cyclically or simultaneously in many environments. This Review discusses these advances with particular focus on their environmental consequences, including the formation of greenhouse gases and the fate of nutrients and contaminants.

Microaerophilic
Microorganisms that oxidize Fe(II) at O_2 concentrations in the tens of micromoles per litre range are microaerophilic Fe(II) oxidizers.

Speciation
Describes the oxidation state and the identity of the coordinating ligands (for example, organic matter, chloride or sulfide).

[1]*Geomicrobiology, Center for Applied Geosciences, University of Tübingen, Tübingen, Germany.*

[2]*School of Earth Sciences, University of Bristol, Bristol, UK.*

[3]*Department of Geological and Atmospheric Sciences, Iowa State University, Ames, IA, USA.*

[4]*These authors contributed equally: Andreas Kappler, Casey Bryce.*

✉*e-mail: andreas.kappler@uni-tuebingen.de*

https://doi.org/10.1038/s41579-020-00502-7

Almost 200 years ago, the German naturalist Christian Gottfried Ehrenberg looked under the microscope at iron-rich mats from freshwater springs and peatlands[1]. The microbially produced stalk-like iron oxide structures he described are now considered characteristic biosignatures for microaerophilic Fe(II)-oxidizing bacteria[2], yet for much of the twentieth century, redox reactions involving iron were presumed to be primarily abiotic processes. In recent years, a great diversity of microorganisms that harvest energy from iron redox transformations has emerged, and our understanding of their physiology, ecology and environmental importance is growing at an ever-increasing pace.

Iron occurs in two main redox states in the environment: ferric iron (Fe(III)), which is poorly soluble at circumneutral pH, and ferrous iron (Fe(II)), which is typically more soluble and therefore more bioavailable. Despite iron having only two naturally occurring redox states, a complex network of biogeochemical interactions, including a tight interplay of biotic and abiotic reactions[3], dictates the speciation, mobility and reactivity of iron in the environment (FIG. 1). The biotic part of iron redox species turnover at circumneutral pH is catalysed by Fe(III)-reducing bacteria as well as microaerophilic, phototrophic and nitrate-reducing Fe(II)-oxidizing bacteria. These can be found in virtually all habitats — terrestrial and aquatic, freshwater and marine, hot and cold, and contaminated and pristine — including many extreme habitats[4]. Iron reduction and oxidation can even occur cyclically[5] or simultaneously[6], with biotic reactions superimposed against a backdrop of abiotic reactions[3]. The bulk geochemistry therefore reflects the net effect of all co-occurring reactions. Unravelling the individual contribution of certain biotic or abiotic processes during iron cycling is extremely challenging[7], despite the availability of various wet-chemical, microscopic, spectroscopic, molecular biological and other analytical methods to follow the abiotic and microbial transformation of dissolved, colloidal and particulate iron redox species (BOX 1).

The redox potentials of diverse Fe(II)–Fe(III) redox couples lie between those of oxidized and reduced carbon, nitrogen, oxygen and sulfur redox species. Consequently, any redox reactions involving iron are tightly linked to these major biogeochemical element cycles (BOX 2). In some cases, this can influence the emission of gaseous products such as N_2O[8] and CH_4 (REF.[9]), which are potent greenhouse gases. Changes in solubility caused by iron redox transformations also indirectly influence the mobility of elements such as phosphorus[10], carbon[11] and metallic elements such as arsenic and cadmium[12,13], with substantial consequences for the fate of nutrients and contaminants in the environment.

Recent advances have revealed the great complexity of the biogeochemical iron cycle. First, much more insight has emerged into the microorganisms and mechanisms behind novel processes in the biogeochemical iron cycle, such as microbial ammonium oxidation and methane oxidation coupled to Fe(III) reduction. Second, processes in the biogeochemical iron cycle that were previously thought to be restricted to distinct geochemical gradients actually overlap spatially and may even compete

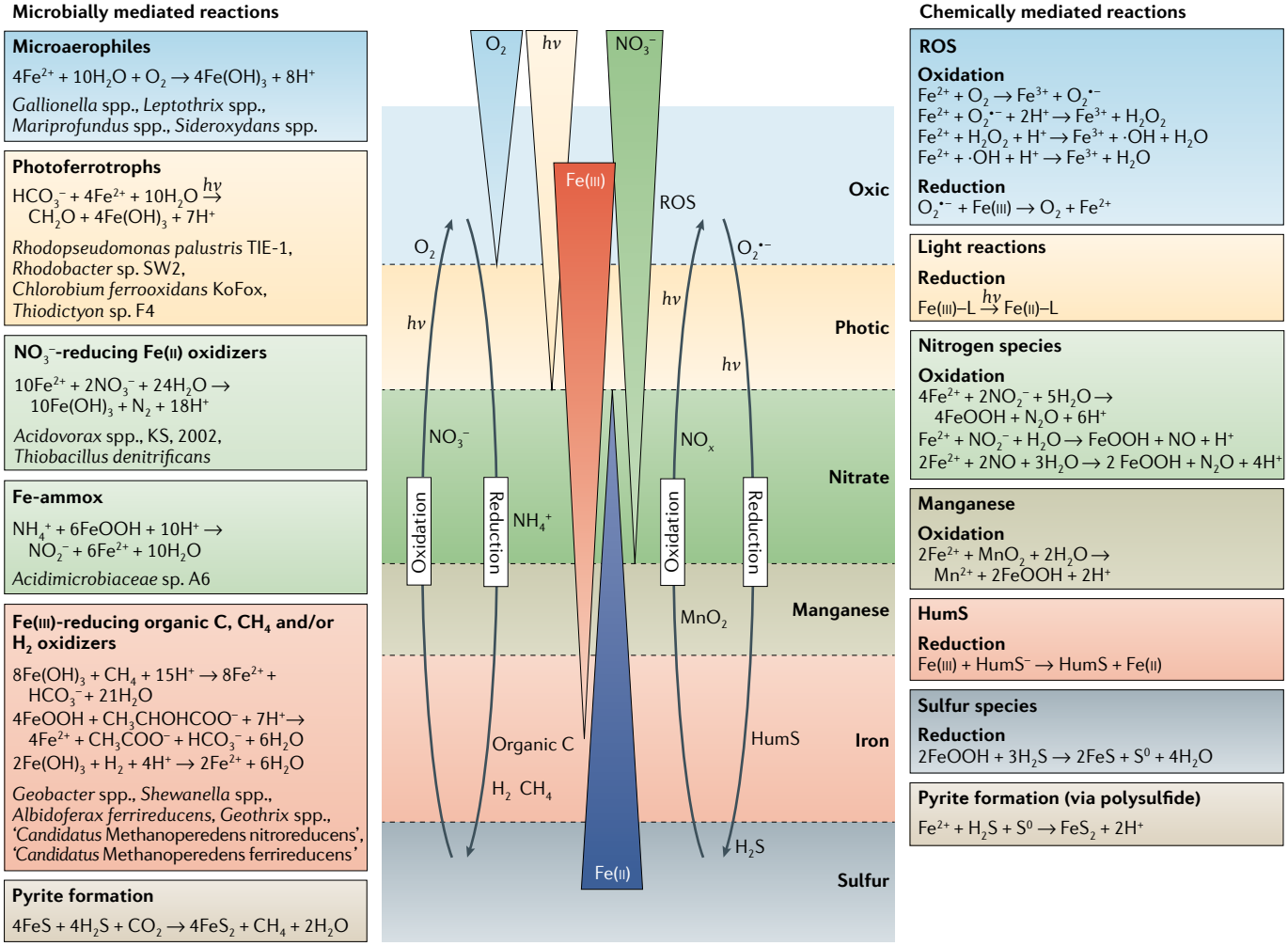

Fig. 1 | **The biogeochemical iron cycle.** All iron redox reactions that occur at circumneutral pH are listed in thermodynamic order, with microbially mediated reactions on the left and abiotic reactions on the right. The central panel depicts gradients of O_2, light, NO_3^-, Fe(II) and Fe(III) that are typical of redox-stratified environments. The coloured panels indicate the sequence in which the different biotic and abiotic reactions are expected to occur on the basis of thermodynamics; however, these often overlap under environmental conditions. Fe-ammox, Fe-dependent ammonium oxidation; HumS, humic substances; ROS, reactive oxygen species. Figure adapted from REF.[3], Springer Nature Limited.

with each other. Third, oxidation and reduction of iron occur cyclically or simultaneously in many environments, leading to so-called cryptic iron cycling, which is not necessarily reflected in the bulk geochemistry.

In this Review, we highlight those recent advances in our understanding of the biogeochemical iron cycle with particular focus on iron reactivity in neutral-pH environments, how anaerobic Fe(III)-reducing or O_2-, light- and NO_x-dependent Fe(II)-oxidizing microorganisms transform iron and how overlapping processes impact the fate of iron and other elements in the environment. We also highlight recent mechanistic insights into metabolisms such as Fe(III)-coupled ammonium and methane oxidation and cryptic iron cycling.

Iron accessibility in the environment

Iron exists in various aqueous and solid phases in the environment at dissolved concentrations from several nanomoles per litre to millimoles per litre and in solids from the microgram per gram range up to high milligram per gram concentrations, which affects the energy that microorganisms can gain from redox processes. The redox potentials (E_h) of iron-bearing phases and their reactivity change considerably as a combined function of ligand and mineral identity, concentrations of dissolved Fe(III) (Fe^{3+}(aq)) and dissolved Fe(II) (Fe^{2+}(aq)), pH, particle size and solid-phase Fe(III)/total Fe ratio (FIG. 2). Faster microbial reduction rates and reactivity are observed for poorly crystalline ferrihydrite over more crystalline iron(III) (oxyhydr)oxide minerals (including iron(III) oxyhydroxides such as goethite or iron(III) oxides such as haematite)[14]; iron(III) (oxyhydr) oxides over clays[15]; the clay NAu-2 over NAu-1 (REF.[16]); and smaller iron(III) (oxyhydr)oxide particles of the same mineralogy[17]. In batch systems, recent innovative electrochemical methods directly showed that the redox potentials of iron(III) (oxyhydr)oxides decrease with progressive microbial reduction[18]. Some Fe(III)-reducing microorganisms can respond to variations in redox potentials by utilizing metabolic pathways that are best

Redox potentials
Redox potential (in millivolts) indicates the thermodynamic driving force for reduction or oxidation, for example, of an Fe(III)–Fe(II) pair.

Ferrihydrite
A poorly crystalline (short-range-ordered) iron(III) oxyhydroxide mineral with a primary particle diameter in the low nanometre range (less than 6 nm), and a resulting large surface area and high reactivity.

Natural organic matter
(NOM). Mixture of organic compounds resulting in nature from the degradation of biopolymers (proteins, lipids, lignin, polysaccharides and so on) stemming from plants, microorganisms and animals.

Nanoparticles
Particles smaller than 100 nm in at least one dimension.

suited to extract the maximum energy yield under any given condition[19]. Besides the redox potential, factors such as activation energies, aqueous speciation and sorption can also affect bioavailability and reduction rates[20]. Complexation of aqueous iron with natural organic matter (NOM) can modify the rate of microbial redox cycling[21], but redox potentials for Fe–NOM complexes are poorly known. NOM complexation is particularly important for Fe(II) oxidation as it can maintain a pool of stable Fe(II) under oxic conditions when it would have otherwise been completely oxidized[22].

Iron minerals also have a wide size distribution in nature, including nanoparticles, colloids and particulates with different reactivities and transport potentials[23]. Colloidal iron minerals have a higher potential for being transported than particulates, making them important vectors for mobilization and transport of iron and associated nutrients and trace metals[24]. Nanoparticles often exhibit the highest reactivity owing to size-dependent quantum confinement effects that enhance solubilities for particles smaller than 100 nm (FIG. 2). The aggregation of colloids and nanoparticles can substantially affect their reactivity and mobility, as shown for microbial reduction of haematite nanoparticles, which showed higher rates for aggregates that are more accessible to electron-transferring proteins[25].

Fe(II) oxidation by oxygen

At circumneutral pH, Fe(II) is thermodynamically unstable in the presence of dissolved oxygen (O_2) at air saturation. Oxidation of Fe(II) coupled to the reduction of O_2 will occur, but the presence of organic

Box 1 | Analysing iron biogeochemistry

Various wet-chemical, microscopic, spectroscopic, molecular biological and other analytical methods are used to follow the abiotic and microbial transformation of dissolved, colloidal and particulate iron redox species.

Mineral identity

- **Mössbauer spectroscopy**. ^{57}Fe-specific absorption of γ-rays provides information on the iron redox state, mineral identity, mineral crystallinity and particle size.
- **X-ray diffraction**. Diffraction of X-rays at the crystal lattice enables mineral identification and provides information about average crystallite size and crystallinity.
- **X-ray absorption spectroscopy**. Synchrotron-based X-ray absorption spectroscopy is used provide information on the iron redox state, mineral identity and binding environment (including iron complexes and minerals).
- **Sequential extraction**. Dissolution by different acids, reducing agents and complexing agents provides information on mineral identity and crystallinity.
- **Fourier-transform infrared spectroscopy and Raman spectroscopy**. Absorption of specific wavelengths (energy) by certain bonds enables the identification of minerals.

Mineral properties and cell mineral associations

- **Wet-chemical titrations**. pH measurements following addition of acids or bases enable the calculation of the charge of particles and aggregates.
- **Dynamic light scattering**. Laser light diffraction is used to determine the hydrodynamic size of particles and aggregates. Coupled to an electrical field (in a Zetasizer), this technique provides information about their surface charge.
- **Transmission electron microscopy (TEM) and scanning electron microscopy (SEM)**. An electron beam is used in scanning or transmission mode to characterize the morphology, size and structure of mineral aggregates, particles, individual crystals and cell–mineral associations. Use in combination with electron diffraction can aid mineral identification.
- **Fluorescence microscopy**. The use of specific fluorescent dyes enables localization, quantification and identification of specific microorganisms and parts of cell–mineral aggregates.
- **Brunauer–Emmett–Teller method**. This method is used to calculate a specific mineral surface area by quantification of sorption of gas molecules or organic compounds.
- **X-ray photoelectron spectroscopy**. Elemental composition at mineral surfaces (~10 nm) is obtained from the kinetic energy of electrons released after irradiation with X-rays.
- **Electrochemical measurements**. Quantification of currents flowing at different redox potentials applied at electrodes enables the calculation of mineral redox potentials or the concentration of redox-active aqueous species.

Compounds associated with minerals

- **Total and dissolved organic carbon**. A total organic carbon analyser (TOC analyser) provides the total amount of carbon present. Following chemical dissolution of iron minerals, a dissolved organic carbon analyser can measure co-eluted carbon.
- **Trace metal and nutrients**. After mineral dissolution, metals, phosphorus and sulfur co-extracted with the minerals can be quantified, for example, by an inductively coupled plasma mass spectrometer.
- **X-ray fluorescence**. This indicates the elemental composition of solid samples.
- **X-ray absorption spectroscopy**. This provides information on the identity, redox state, binding environment and location of mineral-associated organic compounds and metal ions.
- **Energy-dispersive X-ray spectroscopy in SEM and TEM**. Radiation released as a consequence of electrons interacting with the minerals enables the identification and/or quantification of elements.
- **Nanoscale secondary ion mass spectrometry**. A primary ion beam (for example, Cs^+) is used to release secondary ions from the specimen in high (nanometre) resolution and to identify and/or quantify them in a mass spectrometer.

Transformation processes

- **Geochemical, spectroscopic and mineralogical analyses of field samples, and laboratory batch and/or column incubations (microcosms)**. Such analyses, potentially in combination with iron isotope analyses, can quantify and identify dissolved, colloidal and mineral iron species and thus provide quantitative information on the rates and extent of iron transformation.
- **Liquid-cell TEM**. Application of electrons in liquid TEM cells enables monitoring of mineral transformation in real time.

Microorganisms involved in biogeochemical cycling

- **Fluorescence microscopy or flow cytometry**. This enables the quantification of cells stained with fluorescent dyes.
- **Most probable number quantification**. This is a cultivation-based quantification of living Fe(II)-oxidizing or Fe(III)-reducing microbial cells.
- **Quantitative PCR**. Analysis of genes involved in Fe(III) reduction and Fe(II) oxidation enables the identification and estimation of iron-metabolizing microbial activities.
- **Fluorescence in situ hybridization**. The application of specific DNA-binding fluorescent probes enables the localization and quantification of specific microorganisms in laboratory and environmental samples.

Box 2 | **Impact of iron transformation on other biogeochemical cycles**

Despite only one electron being transferred during Fe(II) oxidation or Fe(III) reduction, iron has a disproportionate impact on other major biogeochemical element cycles due to a combination of redox reactions, as well as sorption and co-precipitation.

The redox potentials of the Fe(II)–Fe(III) redox couples lie between those of couples of environmentally relevant carbon, nitrogen, oxygen and sulfur species, which means that iron redox reactions directly influence the redox state of carbon, nitrogen, oxygen and sulfur (FIG. 1). This has important environmental implications, for example by Fe(III) reduction contributing to the mineralization of carbon, or Fe(II) mitigating toxic nitrate and nitrite in wastewaters. Greenhouse gases such as N_2O can be emitted as a consequence of Fe(II) oxidation[8], and Fe(III)-dependent anaerobic oxidation of methane can attenuate CH_4 fluxes[9,193]. Iron redox reactions can also be harnessed for remediation purposes[194]. For instance, the reducing capacity of Fe(II) can be exploited to transform several organic and inorganic contaminants, such as hydrocarbons, pesticides, explosives, azides or heavy metals[191,195].

The redox-dependent solubility of iron at neutral pH also has a strong impact on other element cycles through sorption and co-precipitation. For example, phosphorus strongly binds to iron(III) (oxyhydr)oxides, and thus the mobility of phosphorus is tied to the precipitation and dissolution of iron minerals in sediments, soils and freshwater habitats[10]. Iron minerals are also thought to have a stabilizing effect on organic matter in soils[196] and marine sediments[11]. Iron can also strongly bind trace metals and both organic and inorganic contaminants[194], a function widely exploited in remediation technologies. For example, the ability of iron minerals to sorb arsenic has been widely used in drinking water purification in countries such as Vietnam and Bangladesh[197], but such processes are also useful to trap nickel, copper, zinc and lead[198].

ligands, iron(III) (oxyhydr)oxides and Fe(II)-oxidizing bacteria and the temperature determine the rates and mechanisms[26].

Abiotic Fe(II) oxidation. Abiotic Fe(II) oxidation occurs through two distinct pathways, termed 'homogeneous' and 'heterogeneous'[27]. Homogeneous Fe(II) oxidation involves the reaction of dissolved $Fe^{2+}(aq)$ with O_2. Oxidation of four $Fe^{2+}(aq)$ ions occurs in four, stepwise, one-electron transfers, and produces the reactive oxygen species (ROS) intermediates superoxide ($O_2^{\cdot-}$), hydrogen peroxide (H_2O_2) and hydroxyl radical (·OH) (see Eqs 1–4):

$$Fe^{2+}(aq) + O_2(aq) \rightarrow Fe^{3+}(aq) + O_2^{\cdot-}(aq) \quad (1)$$

$$Fe^{2+}(aq) + O_2^{\cdot-}(aq) + 2H^+ \rightarrow Fe^{3+}(aq) + H_2O_2(aq) \quad (2)$$

$$Fe^{2+}(aq) + H_2O_2(aq) \rightarrow Fe^{3+}(aq) + \cdot OH(aq) + OH^-(aq) \quad (3)$$

$$Fe^{2+}(aq) + \cdot OH(aq) \rightarrow Fe^{3+}(aq) + OH^-(aq) \quad (4)$$

Reactions 1 and 3 are rate-determining steps of the pseudo-first-order reaction. H_2O_2 and O_2 are the main oxidants of Fe(II) in seawater[28], although the concentrations of reactants govern the observed oxidation rates[29]. The rate of abiotic Fe(II) oxidation by O_2 can be slowed when Fe(II) is stabilized by organic ligands[22].

Precipitation of poorly soluble iron(III) (oxyhydr)oxide minerals stimulates rapid abiotic surface-catalysed heterogeneous oxidation of sorbed Fe(II), with the rates being directly proportional to the concentration of solid iron[30].

Microaerophilic Fe(II) oxidation. Microaerophilic, neutrophilic Fe(II)-oxidizing bacteria grow lithoautotrophically using Fe(II) as an electron donor and O_2 as an electron acceptor[31] (see Eq. 5):

$$4Fe^{2+} + 10H_2O + O_2 \rightarrow 4Fe(OH)_3 + 8H^+ \quad (5)$$

These bacteria are members of either the freshwater Betaproteobacteria, of which known genera include *Gallionella*, *Sideroxydans*, *Ferriphaselus*, *Ferritrophicum* and *Leptothrix*[31], or the marine Zetaproteobacteria, for example, *Mariprofundus* spp. and *Ghiorsea* spp.[31–33].

Microaerophilic Fe(II) oxidizers live at mostly aquatic oxic–anoxic interfaces with opposing gradients of O_2 and Fe(II). They are found as microbial mats at groundwater seeps, in water treatment systems and at deep-sea hydrothermal vents[34,35]. They live in freshwater and marine sediments (and also some soils)[36,37]. They colonize oceanic crust, and also live planktonically in redox-stratified water columns[38,39]. Microaerophilic Fe(II) oxidizers must compete with the rapid abiotic oxidation of Fe(II) by O_2 at circumneutral pH[40]. To do so they inhabit niches where the activity of O_2 is well below air saturation. The rates of microaerophilic Fe(II) oxidation outcompete the rates of abiotic oxidation at or below 50 μM O_2 (REF.[26]). Optimum growth of microaerophilic Fe(II) oxidizers occurs at 5–20 μM O_2 (REF.[40]), but growth can still occur at submicromolar concentrations of O_2 (REFS[41,42]).

Oxidation of Fe(II) most likely occurs extracellularly to avoid cell encrustation[43]. A putative fused cytochrome–porin, Cyc2, that is encoded in the genome of all isolates[42,44] is currently considered the most promising candidate as an iron oxidase in microaerophilic Fe(II) oxidizers. This putative iron oxidase was first demonstrated in acidophilic bacteria[45], but was later observed to be highly expressed in the proteome of the neutrophilic marine Fe(II) oxidizer *Mariprofundus ferrooxydans* PV-1 during Fe(II) oxidation[46], and was recently validated to have an important role in neutrophilic Fe(II)-oxidizing mats by metagenomics and metatranscriptomics[44]. The *cyc2* gene is widespread across many lineages of neutrophilic Fe(II)-oxidizing bacteria. Moreover, *cyc2* is highly transcribed in iron-bearing microbial mats and is stimulated by Fe(II) addition[44]. This makes *cyc2* a promising genetic marker for Fe(II) oxidation, although its functionality in neutrophilic Fe(II) oxidizers is still unproven and it is found in the genomes of organisms which have not been described to oxidize Fe(II). There is much still to learn before *cyc2* could be used as a marker gene. The current hypothesis is that electrons from oxidation of Fe(II) at the cell surface are transported to periplasmic cytochromes (Cyc1 or other cytochromes) and then to a cbb_3-type cytochrome oxidase for the reduction of O_2, creating a proton motive force for the generation of ATP[43]. Another possibility is the transfer of electrons from periplasmic cytochromes to another cytochrome and a quinone pool in the inner membrane to finally produce reducing power in the form of NADH[43,47].

Another potential iron oxidase gene (*mtoA*) is present in *Sideroxydans lithotrophicus* ES-1 (REF.[47]), but this gene was found in only a few other genomes of Fe(II) oxidizers[48]. Therefore, Fe(II) oxidation by Cyc2 is

Colloids
Particles smaller than 1,000 nm in at least one dimension that are dispersed in a substance of another physical state (for example, mineral particles in a liquid).

Particulates
Particles larger than 1,000 nm in all dimensions.

Transmission electron microscopy
(TEM). An imaging technique using a beam of electrons transmitted through a thin specimen to obtain an image of the specimen down to atomic resolution, applied in physical, chemical and biological sciences. Can be used, for example, to characterize nanoparticles formed by iron-metabolizing microorganisms.

Scanning electron microscopy
(SEM). An imaging technique using a beam of electrons to scan the surface of a specimen to obtain information about the morphology, topography and surface structure. Applied, for example, to characterize cell–mineral structures of iron-metabolizing microorganisms.

Homogeneous Fe(II) oxidation
The oxidation of reduced iron (Fe(II)) by an oxidant that is in the same physical state (for example, oxidation of dissolved Fe^{2+} by dissolved O_2).

Reactive oxygen species
(ROS). Very reactive compounds with unpaired electrons formed from molecular O_2.

presumably more widespread among microaerophilic Fe(II)-oxidizing bacteria[48].

Some microaerophilic Fe(II)-oxidizing bacteria direct extracellular iron biomineralization onto twisted stalks, tubular sheaths, or granular or dreadlock-like structures[31,32] that consist of poorly crystalline ferrihydrite, lepidocrocite, goethite or akageneite[37,49] and an organic matrix (probably acidic polysaccharides and saturated aliphatic chains of organic carbon)[37]. Besides preventing cell encrustation, the extracellular biominerals were also suggested to fulfil different functions depending on their morphology. Twisted stalks help position bacteria at optimum growth conditions within concentration gradients of O_2 and Fe(II) and to anchor them to surfaces[50]. Dreadlock-like structures are easily shed from cells to help planktonic Fe(II) oxidizers stay suspended in water columns[41].

Microaerophilic Fe(II)-oxidizing bacteria greatly affect Fe(II) oxidation rates, either directly by their metabolism or indirectly by producing iron(III) (oxyhydr)oxides that form a surface catalyst for heterogeneous Fe(II) oxidation[32]. Microaerophilic Fe(II) oxidizers primarily influence the environment by forming unique microenvironments such as microbial mats, influencing and forming gradients of O_2 and Fe(II)[2]. The biomineral mixture of poorly crystalline iron(III) (oxyhydr)oxides and organic constituents functions as carbon and energy sources for Fe(III)-reducing

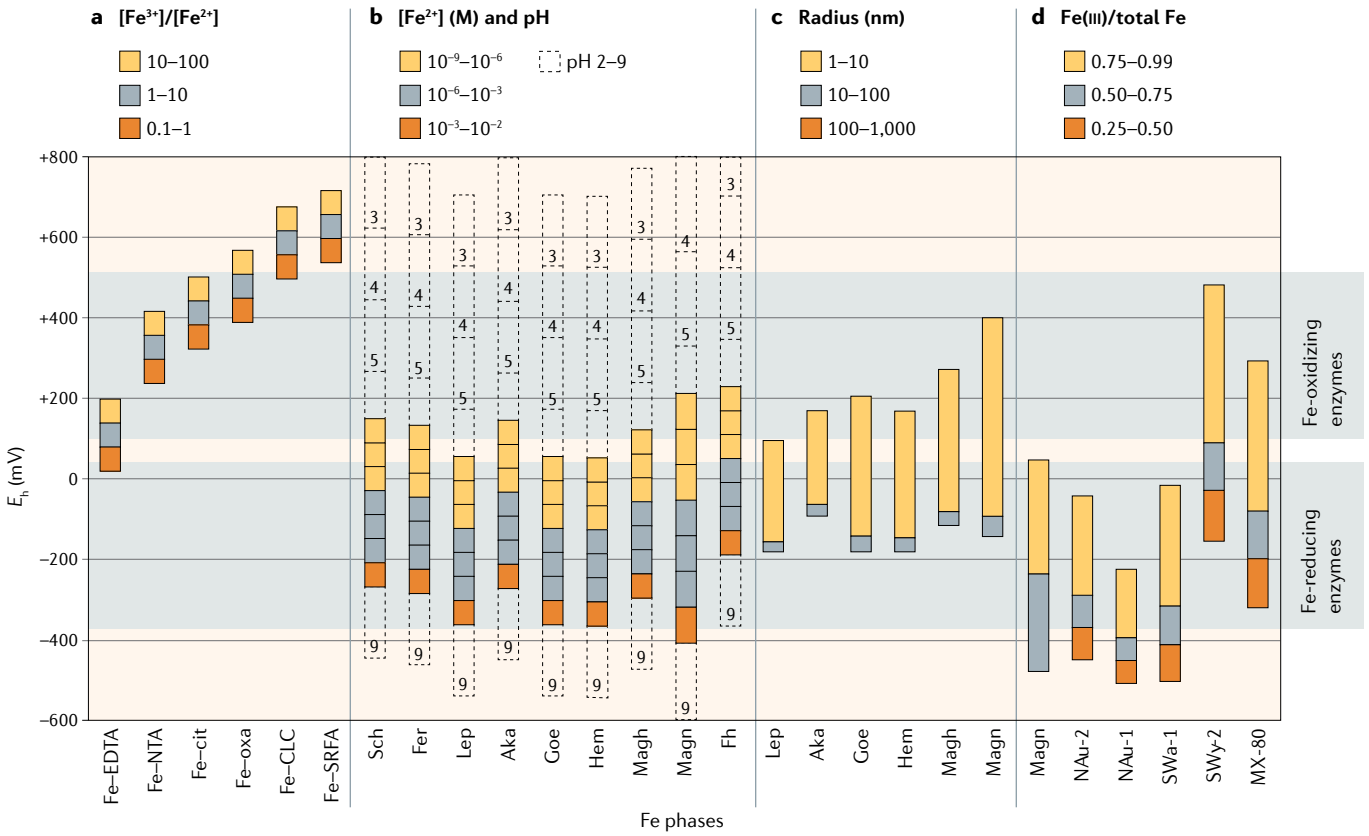

Fig. 2 | **Redox potentials of diverse Fe(II)–Fe(III) redox couples.** Redox potential (E_h) of the Fe(III)–Fe(II) pair for iron-bearing phases at 25 °C, pH 7 and constant Fe^{2+} concentration of 10^{-5} M (unless otherwise specified) showing that iron-bearing minerals and complexes do not have a defined E_h but exist within a range depending on the geochemical parameters and their physical properties. The Fe^{2+} concentration of 10^{-5} M was chosen as an environmentally relevant and representative concentration, typically found in aquatic systems such as sediments (depending on the specific conditions, this value can be higher or lower in nature). The figure is divided into four sections, with E_h values calculated according to the specified variation in Fe^{3+}–L/Fe^{2+}–L concentration ratio of ligand-complexed iron species (panel **a**), Fe^{2+} concentration (coloured boxes with solid outlines) and pH (unfilled boxes with dashed outlines; numbers indicate the pH boundary) (panel **b**), particle radius (panel **c**) and solid-phase Fe(III)/total Fe ratio (panel **d**). Exact ranges of concentration, ratio or particle radius are specified at the top of each panel by the colour code. Shaded horizontal areas correspond to the E_h range of key iron oxidoreductases[69,181–183]. Additional information for E_h determination is as follows. For panel **a**, 1:1 Fe–L complexation and non-dissociative reduction were assumed. Standard redox potentials (E_h^0) were calculated from the stability constant of the one-electron reduction of Fe^{3+} to Fe^{2+} (log K = 13) and the stability constants of the respective Fe^{3+}–L and Fe^{2+}–L complexes, as obtained from the ThermoChimie database (version 10a)[184] (for ethylenediaminetetraacetic acid (EDTA), nitriloacetic acid (NTA), citrate (cit) and oxalate (oxa)) or from REF.[185] (for natural organic matter extract from sugar cane (CLC) and Suwannee River fulvic acid (SRFA); conditional log K values at pH 8.1 in seawater). For panel **b**, E_h^0 was obtained or calculated from the standard Gibbs free energy of formation (ΔG_f^0) from REFS[186–188] and converted to E_h as a function of Fe^{2+} concentration (at constant pH 7) or as a function of pH (at constant Fe^{2+} concentration of 10^{-5} M). For schwertmannite (Sch), a constant SO_4^{2-} concentration of 10^{-4} M is assumed. For panel **c**, E_h^0 was corrected for increased surface energy of small particles through published mineral-specific enthalpies of hydrated surfaces (ΔH_s^h)[186,189] and molar volumes[190], assuming geometric surface area. For panel **d**, E_h values were determined directly at pH 7–7.5 through electrochemistry for 10–20 nm magnetite (Magn) particles and various clay reference materials (NAu-2, NAu-1, SWa-1, SWy-2 and MX-80)[191,192]. Aka, akageneite; Fer, feroxyhyte; Fh, ferrihydrite; Goe, goethite; Hem, haematite; Lep, lepidocrocite; Magh, maghemite.

Lepidocrocite
A ferric iron oxyhydroxide polymorph (γ-FeOOH) with a yellow to reddish brown colour.

Goethite
A ferric iron oxyhydroxide polymorph (α-FeOOH) known for its use as a paint pigment and named after the poet Johann Wolfgang von Goethe.

Akageneite
A chloride-containing ferric iron oxyhydroxide polymorph (β-FeOOH) that typically forms in marine environments.

Heterogeneous Fe(II) oxidation
The oxidation of iron (Fe(II)) by an oxidant that is in a different physical state (for example, oxidation of sorbed Fe(II) by dissolved O_2).

Voltammetric microelectrodes
Electrodes with tip diameters in the micrometre range (the potential at the working electrode is varied and the resulting current is recorded). Such electrodes can be used to identify and quantify iron redox species with high spatial resolution (for example, in sediments).

c-type cytochrome
A protein that contains haem as a prosthetic group and is involved in oxidation and reduction reactions inside and outside the microbial cell.

Extracellular polymeric substances
Organic molecules consisting of polysaccharides and proteins, but also DNA and lipids, purposefully released by microorganisms into the environment (for example, during biofilm formation).

bacteria or other bacteria[31], especially because nutrients, organic matter and heavy metals can also adsorb or co-precipitate with those highly reactive biominerals[37,51].

Parsing abiotic from biotic circumneutral Fe(II) oxidation. Biotic and abiotic Fe(II) oxidation reactions occur in parallel, which makes identifying the occurrence and quantitative contribution of microaerophilic bacteria to overall Fe(II) oxidation challenging. Microbial Fe(II) oxidation can account for 50–80% of the total Fe(II) oxidation over a wide range of microoxic conditions[31,32]. Voltammetric microelectrodes have been applied in field settings to identify zones where Fe(II) and O_2 concentrations should support Fe(II)-oxidizing bacteria[35]. Gradient tubes have long been used to enrich Fe(II)-oxidizing bacteria, but can also be used to distinguish biotic from abiotic Fe(II) oxidation by comparing Fe(II) concentrations measured with voltammetric microelectrodes in gradient tubes inoculated with or without Fe(II) oxidizers[26,52]. Recently, a liquid culture microcosm approach was applied to quantify the effect of heterogeneous Fe(II) oxidation on biotic versus abiotic Fe(II) oxidation at various O_2 concentrations[40].

As shown for a peatland drainage and groundwater discharge channel, the in situ rates of microbial Fe(II) oxidation depend on water flow leading to advection and turbulent mixing[46], and those reports emphasize that ex situ experiments in laboratory settings risk underestimating the oxidation rates that actually occur in nature[46]. Rates have recently been quantified by modelling iron concentrations as a function of transit time through a small stream, revealing seasonal differences in the contribution of biotic processes to Fe(II) oxidation[53]. Long-range correlations of temporal fluctuations of redox potential can also distinguish bacterial from abiotic Fe(II) oxidation in incubation of field samples[54].

Light-induced iron redox reactions

Iron redox cycling often occurs at oxic–anoxic interfaces, but light-driven reactions can also drive iron cycling, even under anoxic conditions. These processes are relevant to aquatic systems, as photosynthetically active radiation penetrates more than 100 m in water or 5–6 mm in sediments[55].

Microbial phototrophic Fe(II) oxidation. Photoautotrophic Fe(II)-oxidizing bacteria (photoferrotrophs) are primary producers that use light energy and electrons from Fe(II) to fix bicarbonate into organic carbon (see Eq. 6):

$$HCO_3^- + 4Fe^{2+} + 10H_2O \xrightarrow{h\nu} CH_2O + 4Fe(OH)_3 + 7H^+ \quad (6)$$

They were first described by Widdel et al.[56], but the existence of such a metabolism was previously hypothesized[57]. Photoferrotrophy has thus been implicated as an oxygen-independent mechanism for Fe(II) oxidation and deposition of Precambrian-aged banded iron formations from the oceans[56], as well as in primary productivity[58].

Isolated photoferrotrophs comprise three taxonomic groups. Purple sulfur bacteria (PSB) belong to the phylum Gammaproteobacteria, represented by *Thiodictyon* sp.[59]. Purple non-sulfur bacteria (PNSB) are members of the phylum Alphaproterobacteria and include *Rhodobacter ferrooxidans* SW2 (REF.[60]), *Rhodopseudomonas palustris* TIE-1 (REF.[61]) and two marine strains (*Rhodovulum iodosum* and *Rhodovulum robiginosum*)[62]. Green sulfur bacteria (GSB) are all members of the family Chlorobiaceae, and are represented by *Chlorobium ferrooxidans* strain KoFox, the dominant member of an enrichment culture[63], the first pelagic isolate *Chlorobium phaeoferrooxidans*[64] and the marine *Chlorobium* sp. strain N1 (REF.[65]).

Two protein-encoding operons are known to catalyse Fe(II) oxidation in PNSB. The *pioABC* operon is required by *R. palustris* TIE-1 for phototrophic Fe(II) oxidation[66]. *pioB* encodes a putative outer membrane porin that may transport Fe(II) into or Fe(III) out of the periplasm. PioA, a periplasmic decahaem *c*-type cytochrome, forms a complex with the outer membrane porin PioB and facilitates uptake of extracellular electrons across the outer membrane[67]. PioC, a high-potential iron–sulfur protein, is thought to subsequently shuttle electrons to the photosynthetic reaction centre[68]. The *foxEYZ* gene cluster, which is not a *pioABC* homologue, stimulates light-dependent Fe(II) oxidation in *R. ferrooxidans* SW2 (REF.[59]). Fe(II) is thought to be transported by an inner membrane protein encoded by *foxZ*, whereas *foxY* is likely to have a role in electron transfer. FoxE is a dihaem cytochrome *c* suggested to function as an iron oxidoreductase[69], and it is required for light-dependent Fe(II) oxidation[59].

The GSB *C. phaeoferroxidans* and the recently isolated *Chlorobium* strain N1 both encode Cyc2 (REFS[70,71]), an outer-membrane protein whose homologues in oxygen-dependent Fe(II)-oxidizing bacteria are thought to directly accept electrons from Fe(II)[43] (see earlier).

Photoferrotrophs produce poorly crystalline ferric oxyhydroxide minerals, which mature into goethite or lepidocrocite[72]. Photoferrotrophs do not seem to become encrusted in minerals and do not form elaborate structures as microaerophilic Fe(II) oxidizers do[73]. Proposed strategies to localize precipitation away from the cell surface include lowering pH around the cell[74], using lipopolysaccharide fibres to template biomineralization[72] or secretion of organic iron-binding ligands, such as extracellular polymeric substances, that help to bind and/or transport Fe(III)[75].

Photochemically induced iron cycling. Photochemical Fe(III) reduction has a major role for iron availability in sunlit aquatic and sedimentary environments by converting iron into more reactive and potentially more bioavailable phases[76]. Fe(III) photoreduction occurs by two major mechanisms: either by direct ligand-to-metal charge transfer (LMCT)[77] or indirectly by photochemically produced radicals[78]. The mechanism depends on the speciation of iron, whereas the rates and extent of Fe(III) photoreduction depend on the wavelength and intensity of light, pH, temperature and ionic strength[79].

At circumneutral pH, most dissolved Fe(III) is complexed by organic ligands (Fe(III)–L) in the form of 0.02–0.4 μm colloids[76], which drastically increases Fe(III) solubility. The organic ligand pool in natural waters may

Humic substances
Stable organic molecules that are redox active and thought to form by humification; that is, the transformation of biomolecules (including lignin, proteins and polysaccharides). This formation theory has been questioned and is being gradually replaced by a soil continuum model.

Siderophores
Organic compounds produced and released by microorganisms in order to make otherwise poorly soluble Fe(III) ions bioavailable for the cells and to facilitate their uptake.

Chemolithoautotrophic
Describes microorganisms that use energy from a chemical reaction of inorganic compounds (for example, oxidation of Fe(II)) to fix carbon from CO_2 into biomass.

Mixotrophs
Microorganisms using an inorganic electron source (for example Fe(II)) in addition to an organic compound for their metabolism are termed mixotrophs, i.e. mixotrophic microorganisms.

contain polysaccharides, humic substances or siderophores with different functional groups[68]. Fe(III)–organic complexes containing an α-hydroxy carboxylic acid group can undergo light-induced LMCT reactions[80] — those ligands can also cause light-induced dissolution of Fe(III) colloids[81]. The LMCT reaction produces Fe(II), oxidizes organic ligands to CO_2 and/or yields organic molecules with altered binding properties[82].

Alternatively, Fe(III) can be reduced by superoxide produced from photochemical reactions of NOM with O_2 (REF.[83]). Photochemical reactions of NOM are the primary pathway for ROS production in sunlit surface waters[83]. The relative importance of LMCT reactions versus superoxide-mediated Fe(III) photoreduction in the environment is still a subject of debate[84], and the contributions of either process are likely to be determined by the dominant Fe(III) species and the type of NOM[82,84]. Photolabile Fe(III)–organic complexes favour LMCT reactions, whereas Fe(III) bound to photostable complexes or present as iron(III) (oxyhydr)oxides favours superoxide-mediated Fe(III) reduction[84].

Fe(III) can also be reduced by photic zone-dwelling phytoplankton. Marine phytoplankton produce extracellular superoxide[85], leading to ROS-driven Fe(III) reduction, although superoxide is also produced by diverse bacteria below the photic zone[86]. Cyanobacteria are able to reduce Fe(III) to Fe(II) enzymatically[87], in addition to a superoxide-mediated pathway[84]. These mechanisms likely enhance iron bioavailability to cyanobacteria, and their contribution to Fe(II) production in the photic zone of iron-rich waters may be substantial[88].

Integrating light-dependent abiotic and microbial iron oxidation. Despite fast Fe(II) oxidation kinetics in oxygenated, circumneutral pH waters, Fe(III) photoreduction leads to increased Fe(II) concentrations in sunlit surface waters following diel cycles[89] as well as increased Fe(II) concentrations in the upper millimetres of light-illuminated sediments[90,91]. Photoreduction can provide a source of Fe(II) to photoferrotrophs and other Fe(II)-oxidizing bacteria[92], which in turn provide Fe(III) for microbial Fe(III) reduction[93]. Light-driven iron cycling is ultimately limited by the light penetration depth. Photosynthetic organisms stratify according to light quantity and quality: oxygenic phototrophs generally need about 1% of surface photosynthetically active radiation[94], whereas photoferrotrophic PSB and PNSB as well as GSB can thrive with less light and prefer anoxic conditions[95]. GSB photoferrotrophs should live deepest, as they use shorter wavelengths than PSB and PNSB, and they are adapted to extreme light limitation[96].

Fe(II) oxidation by nitrogen species

As a consequence of environmental nitrogen cycling processes, and amplified by intensive fertilizer use over the past decades, nitrate co-occurs with Fe(II) in many habitats, such as in aquifers, stratified water bodies or in the top few anoxic millimetres and centimetres of sediments. Microbial and abiotic redox reactions between dissolved and solid-phase Fe(II) species and the oxidized nitrogen compounds nitrate and nitrite can facilitate nitrate removal and enhance the production of the greenhouse gas N_2O.

Microbially mediated nitrate-reducing Fe(II) oxidation. Oxidation of Fe(II) coupled to reduction of nitrate to N_2 (see Eq. 7) or to ammonium (dissimilatory nitrate reduction to ammonium; see Eq. 8) under anoxic conditions was first described in 1996 (REF.[97]).

$$10Fe^{2+} + 2NO_3^- + 24H_2O \rightarrow 10Fe(OH)_3 + N_2 + 18H^+ \quad (7)$$

$$8Fe^{2+} + NO_3^- + 21H_2O \rightarrow 8Fe(OH)_3 + NH_4^+ + 14H^+ \quad (8)$$

Several strains capable of catalysing nitrate reduction coupled to Fe(II) oxidation (NRFeOx) have been reported, but in recent years it has become evident that only a minority represent chemolithoautotrophic NRFeOx[98], where in this case Fe(II) oxidation is coupled to energy generation by nitrate reduction and to CO_2 fixation for biomass production[99]. Chemolithoautotrophic NRFeOx has been demonstrated unambiguously for the enrichment culture KS[99], for another enrichment culture obtained from a nitrate-contaminated groundwater aquifer (Jakus et al., manuscript in preparation) and in marine sediments[100]. However, in most cases nitrate reduction is instead coupled to oxidation of background or cell-stored carbon, and Fe(II) oxidation is catalysed by nitrite and other reactive nitrogen species produced as by-products of heterotrophic denitrification in a process termed 'chemodenitrification'[98]. Some of the published strains may also be true mixotrophs and oxidize both Fe(II) and organic compounds enzymatically with an energetic benefit from Fe(II) oxidation. Many heterotrophic denitrifiers produce reactive nitrogen species that lead to abiotic Fe(II) oxidation and N_2O formation[101], and this is likely to be environmentally important, including for the greenhouse gas budget[102,103].

For several studies with isolated strains and environmental samples, the extent of enzymatic Fe(II) oxidation and chemodenitrification remains unclear. As both types of microorganisms, the ones catalysing NRFeOx and chemodenitrifiers, use the same enzymatic pathways for nitrate reduction, they cannot be distinguished on the basis of genomic characteristics. The only genomic indicator could be the presence of an iron(II) oxidase. However, the mechanism responsible for the oxidation of iron is controversial even in the most well-studied chemolithoautotrophic culture growing by NRFeOx; that is, culture KS[104]. Recent attempts to analyse nitrogen and oxygen isotope composition in oxidized and reduced nitrogen species, before and after reaction with Fe(II) in the presence of active microorganisms have shown potential for disentangling the complex network of coupled biotic and abiotic Fe–N redox reactions[105], but more work is needed to solve this conundrum.

Microbial mineral oxidation with nitrate. Oxidation of iron(III) sulfide (FeS) and pyrite (FeS_2) has been shown to be coupled to reduction of nitrate[106]. *Thiobacillus denitrificans*, various members of the genera *Acidovorax* and *Geothrix*, and a *Marinobacter*-related isolate have been suggested to catalyse these reactions[106,107]. However, at

Fe(III) reducers
Microorganisms that specialize in gaining energy by coupling Fe(III) reduction with the oxidation of an electron donor (for example, an organic compound).

least some of the observed FeS and FeS_2 oxidation can probably be attributed to either abiotic pyrite oxidation by microbially produced nitrite during acidic extraction of the iron species (when nitrite is formed from nitrate reduction coupled to oxidation of reactive elemental sulfur or organic carbon; BOX 3)[108] or oxidation by Fe(III) formed from oxidation of small amounts of Fe^{2+}(aq) (REF.[109]).

Additionally, microbial enzymatic nitrate reduction can be coupled to oxidation of Fe(II) in clays (for example, illite[110], smectites[111] or biotite[112]), although a contribution of abiotic oxidation of the Fe(II) in the clays by nitrite or by Fe(III) cannot be ruled out in these cases.

Microbial mineral formation by nitrate-reducing Fe(II)-oxidizing bacteria. Oxidation of dissolved Fe^{2+}, Fe(II) complexed by organic matter, or Fe(II) minerals (for example, vivianite or siderite) by bacteria catalysing NRFeOx at neutral pH leads to the formation of poorly soluble Fe(III)[98]. This was shown to precipitate, depending on the geochemical and physical conditions in the growth medium (for example, the presence of NOM, ions and nucleation sites, or pH and temperature), as poorly crystalline ferrihydrite-like iron(III) oxyhydroxide, as iron(III) phosphate, as more crystalline goethite or as mixed-valence Fe(II)–Fe(III)-containing green rust[113,114]. Depending on the bacterial strain or strains involved and the resultant extent of either enzymatic, chemolithoautotrophic Fe(II) oxidation[115] or abiotic Fe(II) oxidation by chemodenitrification[72], these minerals were found in close association with the cells forming cell–mineral aggregates. In many cases the minerals were associated with extracellular polymeric substances, on the cell surface or even in the cell periplasm. Occasionally minerals even completely encrust the cells. The formation of nanoparticulate Fe(III) minerals with large surface areas and binding capacities by nitrate reduction coupled to iron oxidation can have important implications for the fate of nutrients and pollutants[116].

Box 3 | Pitfalls in iron analyses

Most studies of iron cycling rely to some extent on wet-chemical extractions to dissolve minerals and to stabilize Fe(II) and Fe(III) concentrations for subsequent analyses. Numerous extraction protocols exist, many involving dissolution with various strengths of acid[199]. However, care must be taken to avoid common pitfalls related to sample acidification. For example, solubilization of iron(III) (oxyhydr)oxides under acidic conditions can lead to electron transfer from reduced species such as hydrogen sulfide or natural organic matter to aqueous Fe^{3+}, which has a more positive redox potential, leading to Fe(III) reduction and an overestimation of the Fe(II) content of the sample.

Problems can also occur in the acidification of samples containing nitrite. Nitrite becomes protonated to nitrous acid at low pH, and further decomposes to NO_2 and NO, which rapidly oxidize Fe(II)[177]. This results in underestimation of dissolved Fe(II) concentrations. In this case, sulfamic acid, which quenches nitrite, has been proposed to be more suitable for sample preservation[177]. However, this will be inadequate to preserve the redox state of carbonate-rich samples due to pH buffering. A combination of sulfamic acid and hydrochloric acid is suggested to preserve Fe(II)/Fe(III) ratios in high-nitrite, high-carbonate samples[200].

Although Fe(II)/Fe(III) ratios are generally considered to be stable at low pH, oxidation by O_2 occurs within minutes in 6 M HCl at 70 °C but is not seen in 1 M HCl at ambient temperatures[201]. This is because Fe–HCl complexes are rapidly oxidized at increased temperatures. Acidity and temperature therefore need to be factored into any decision about whether to conduct extractions under oxic or anoxic conditions.

Strong acid extractions aim to dissolve minerals. Acid extraction of adsorbed Fe(II) on iron(III) (oxyhydr)oxides is generally accomplished by incubation with 1 M sodium acetate at pH 4.85 or 0.5 M HCl, with the latter extractant able to dissolve some of the solid[202]. However, 1 M sodium acetate will also partially dissolve iron carbonates[203], which would overestimate adsorbed iron in carbonate-bearing samples. Use of extraction-independent techniques (for example, X-ray diffraction or Mössbauer spectroscopy) to verify the types of iron minerals can provide context to interpret results.

Even if the redox state can be accurately preserved during acid extraction, numerous compounds interfere with spectrophotometric methods typically used for iron quantification. These methods involve the use of complexing agents that form stable, coloured complexes with dissolved Fe(II), such as ferrozine[204] or phenanthroline[205]. The reaction must be well buffered, as the absorption of the Fe(II)–ferrozine complex is attenuated below pH 4 and above pH 10 (REF.[204]). Reduction of Fe(III) complexed with organic matter by hydroxylamine can also be incomplete in the presence of humic substances, leading to underestimation of total iron and therefore inaccurate Fe(II)/Fe(III) ratios[206]. In this case, an alternative quantification method for total iron may be warranted. The accuracy of the ferrozine assay is also strongly impacted by heavy metals such as copper and cobalt[204] that also form complexes with ferrozine. For well-characterized samples, relevant metals should be included in the standards.

Fe(III) oxidation by Mn(IV)

Manganese is present in the environment as reduced, dissolved Mn(II) or in the form of manganese(IV) oxide minerals. The importance of Mn(III) as an intermediate in manganese redox cycling was recently revealed[117]. Manganese often co-occurs with iron. These elements influence each other's redox speciation and reactivity, with consequences for other biogeochemical cycles[118]. Fe(II) is abiotically oxidized by manganese(IV) oxides through a surface-controlled inner-sphere electron transfer process[119] (see Eq. 9) (FIG. 1):

$$MnO_2 + 2Fe^{2+} + 2H_2O \rightarrow Mn^{2+} + 2FeOOH + 2H^+ \quad (9)$$

Because of its more positive redox potential, Mn(IV) reduction is generally expected to occur first, then Fe(III) reduction, and as a consequence, reduction of Mn(IV) minerals is spatially separated from reduction of Fe(III) minerals (for example, in stratified lake sediments[120]). However, in many environments manganese cycling and iron cycling are tightly coupled; for example, in rice paddies, where steep redox gradients exist on small scales[121].

Fe(III) reduction

Microbial Fe(III) reduction. Fe(III)-reducing bacteria couple the reduction of ferric iron with the oxidation of organic or inorganic electron donors. This capability has been demonstrated for different microorganisms in almost every anoxic environment on Earth. Examples of Fe(III) reducers include *Geobacter* spp.[122], *Shewanella* spp.[123], *Albidoferax ferrireducens*[124], *Geothrix fermentans*[125] and hyperthermophilic archaea[126].

The electron donors used by Fe(III) reducers include fatty acids, carbohydrates, amino acids, aromatic compounds and dihydrogen (H_2)[20]. Fe(III) reducers can use complexed dissolved Fe(III) as an electron acceptor. At circumneutral pH and in the absence of organic ligands, Fe(III) is more typically present as either short-range-ordered mineral phases (for example, ferrihydrite) or crystalline minerals (for example, goethite, haematite and magnetite). Although a number of Fe(III) mineral phases have been shown to function as electron acceptors for *Geobacter sulfurreducens*, including

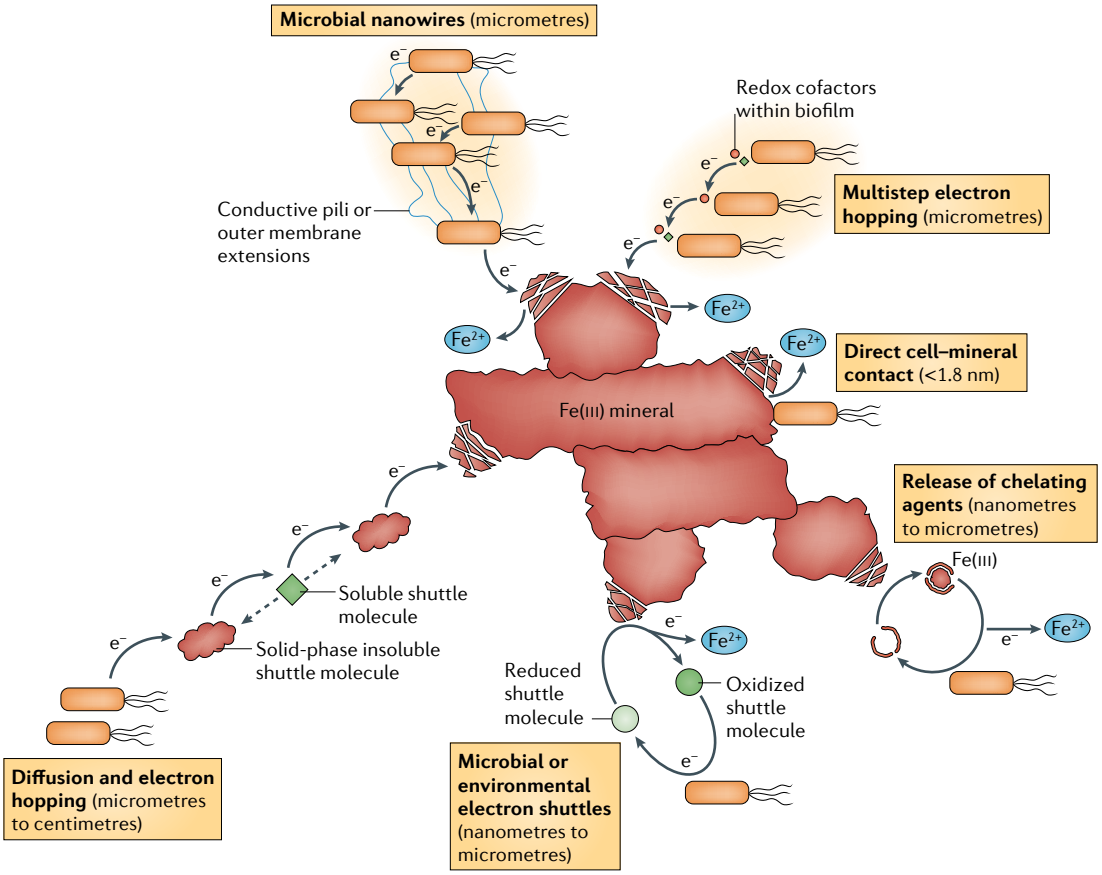

Fig. 3 | **Electron transfer mechanisms from microorganisms to Fe(III) minerals.** This schematic summarizes the strategies utilized by Fe(III) reducers to access solid iron as an electron acceptor. Over short distances, they can directly transfer electrons to surfaces with which they are in contact. Alternatively, they can utilize chelating agents or microbial/environmental redox-active electron shuttles to facilitate electron transfer. Within biofilms, they may assemble electrically conductive pili or outer membrane extensions to transfer electrons, or they can pass the electrons through the biofilm via redox cofactors in a process termed 'electron hopping'. In a combination of diffusion of soluble redox-active shuttles and electron hopping via insoluble (solid-phase) shuttles, microorganisms can facilitate Fe(III) reduction over long distances (centimetres). Figure adapted from REF.[3], Springer Nature Limited.

haematite, lepidocrocite, feroxyhyte, akageneite and schwertmannite[14], the energy gained by such electron transfer varies depending on the mineral (FIG. 2).

The identity of the minerals produced by microbial Fe(III) reduction depends on a number of factors, including temperature, reduction rate and the presence of anions such as bicarbonate or phosphate, and can lead to the formation of siderite, vivianite, magnetite, green rust or, via Fe(II)-catalysed transformation of ferrihydrite, even to goethite[127]. Equation 10 indicates the formation of magnetite formed by the reduction of an iron(III) oxyhydroxide coupled to the oxidation of acetate as is typical of *G. sulfurreducens*.

$$CH_3COO^- + 24FeOOH \rightarrow 8Fe_3O_4 + 2HCO_3^- + 12H_2O + H^+ \quad (10)$$

Another well-studied group of Fe(III)-reducing bacteria are members of the Shewanellacae, in particular strain *Shewanella oneidensis* MR-1, which was isolated in the 1990s[123] and can reduce ferric iron with H_2, formate or lactate as an electron donor.

Electron transfer strategies. Fe(III) reducers, notably *Shewanella* and *Geobacter* species, face the challenge of low solubility of their electron acceptor. This prevents uptake of iron into the cells and requires them to use various electron transfer mechanisms for dissimilatory Fe(III) reduction (FIG. 3), which are described below. The first mechanism involves direct contact between proteins associated with the outer cell wall and the Fe(III) mineral surface. This mechanism relies on electrons that originate from intracellular catabolism to be transferred to *c*-type cytochromes localized on the cell surface, which then mediate extracellular electron transfer to iron(III) (oxyhydr) oxides[128]. The differences reported between the electron transport pathways of *S. oneidensis* and *G. sulfurreducens*[129], and even within the *Geobacter* species[130], suggest that there are several biochemical pathways available for direct-contact Fe(III) mineral reduction.

The second mechanism requires the use of conductive organic pili-like structures (microbial nanowires) to transfer electrons to the surface of the Fe(III) minerals[131]. Extracellular, conductive structures are thought to be constructed by many bacteria and even archaea[132]. The most widely studied are the electrically conductive pili

of *G. sulfurreducens* and *Geobacter metallireducens*. *G. sulfurreducens* constructs conductive pili from the type IV pilin monomer protein PilA[133–135]. There is a substantial and growing body of evidence that these pili in *G. sulfurreducens* (and the related *G. metallireducens*) facilitate transfer of electrons over distances of around 20 μm to extracellular electron acceptors, including iron(III) oxides[136]. *Shewanella* species can also transfer electrons across similar distances using extracellular appendages formed by extensions of the outer membrane and periplasm, facilitated by multihaem cytochromes[137,138]. Considerable advancements have been made in recent years in establishing the molecular underpinnings of electron transfer via these appendages; however, it remains the subject of lively debate[132].

In addition, redox-active electron shuttles such as dissolved or solid-phase NOM (including humic substances), redox-active mineral particles, sulfur compounds, self-made redox mediators or mediators produced by other microorganisms can be used to transfer electrons between the intracellular electron transfer chain and the distant solid mineral phases[139–141] (FIG. 3). The principle behind this mechanism is that the microorganisms first reduce the electron shuttle (for example, oxidized NOM or oxidized sulfur species) in an enzymatic reaction, the shuttle becomes reduced (reduced NOM or reduced sulfur species) and then transfers the electron to the terminal electron acceptor, for example poorly soluble Fe(III) minerals, in an abiotic reaction. The electron shuttles become reoxidized during this second abiotic part of the process and can serve again as an electron acceptor for the microorganisms, thus sustaining the cyclic electron shuttling process.

For electron shuttling, microorganisms have been shown to use dissolved and solid-phase NOM[124,139]. These includes microorganisms with different physiology (for example, fermenters, methanogens, sulfate reducers and halorespirers) from diverse environments, such as lake and marine sediment and pristine and contaminated wetland sediments[124,142,143], ultimately making all of them indirect Fe(III) reducers[144]. In addition to the abiotic reactions of Fe(III) minerals with NOM, reduced sulfur species such as sulfide are also able to reduce iron(III) (oxyhydr)oxides abiotically[145].

S. oneidensis excretes self-made redox-active mediators (flavins) as electron shuttles[146,147]. Other *Shewanella* strains, such as *Shewanella alga* strain BrY, were shown to also use Fe(III) chelators[148], thereby facilitating the use of Fe(III) as an electron acceptor. Flavins may even enhance direct electron transfer[128], and have an effect on the measured redox potential in sediments[149]. It was recently shown that anthraquinone-2,6-disulfonic acid (AQDS), a model compound for redox-active moieties in NOM, could support long-range electron transfer of at least 2 cm through a combination of AQDS molecular diffusion and electron hopping from reduced to oxidized AQDS molecules[150,151]. Iron reducers have also been shown to harness the electron-accepting capabilities of the mixed-valence iron oxide magnetite to replace biological electron transfer proteins[152]. In that study, a wild-type strain of *G. sulfurreducens* exhibited lower expression of a specific multihaem *c*-type cytochrome, OmcS, which is responsible for electron transfer, when incubated with nanoscale magnetite compared with incubation without magnetite. This observation suggests that solid iron minerals such as magnetite might be able to function in a manner similar to cytochromes in microbial extracellular electron transfer.

The final mechanism describes non-reductive dissolution of iron(III) (oxyhydr)oxides by microbial secretion of organic ligands (Fe(III) chelators), which leads to the release of more readily reducible soluble Fe(III) complexes[153].

Microbial Fe(III) reduction coupled to methane and ammonium oxidation. In recent years, the role of Fe(III) reduction in promoting the oxidation of methane and ammonium has received increasing attention. Oxidation of these compounds is most thermodynamically favourable with O_2 as an electron acceptor, but anaerobic methane oxidation can occur in anoxic environments coupled to the reduction of Fe(III), Mn(IV), nitrate or sulfate as electron acceptors[154].

Fe(III)-dependent anaerobic oxidation of methane (AOM) (see Eq. 11) has been inferred from geochemical and isotopic evidence in freshwater[155] and marine[9] sediments, paddy fields[156], stratified lakes[157] and contaminated aquifers[158,159]. Given the abundance of Fe(III) in the environment, AOM coupled to Fe(III) reduction can represent a substantial methane sink[9].

$$CH_4 + 8Fe(OH)_3 + 16H^+ \rightarrow CO_2 + 8Fe^{2+} + 22H_2O \quad (11)$$

Anaerobic methane-oxidizing (ANME) archaea similar to the ANME-2 lineage have been identified to be responsible for Fe(III) reduction[160]. ANME archaea may utilize conductive nanowires resembling pili-like structures formed by *Geobacter* consortia[161].

In freshwater sediment bioreactors, '*Candidatus* Methanoperedens nitroreducens' was shown to reduce iron(III) citrate coupled to AOM[162]. More recently, '*Candidatus* Methanoperedens ferrireducens' was shown to conduct AOM in an Fe(III)-dependent manner, and may use multihaem cytochromes to facilitate extracellular dissimilatory Fe(III) reduction[163].

Microbial Fe(III) reduction can also be coupled to ammonium oxidation and is colloquially known as 'Fe-ammox' (see Eq. 12).

$$NH_4^+ + 6FeOOH + 10H^+ \rightarrow NO_2^- + 6Fe^{2+} + 10H_2O \quad (12)$$

This process occurs in anoxic, iron-rich and water-saturated systems such as riparian[164], forested[165] and coastal[166] wetlands and in rice paddy soils[167]. It has also been described in forest soils[168] and sewage sludge[169]. To date, only one microorganism, *Acidimicrobiaceae* sp. A6, has been isolated that oxidizes NH_4^+ to NO_2^- under Fe(III)-reducing conditions[170]. Fe-ammox can also result in the conversion of NH_4^+ to NO_3^- (REF.[171]) or, in the most thermodynamically favourable option, to N_2 gas[168]. However, the individual microorganism or consortium responsible for this is as yet unknown[154]. In addition

to driving transformation of Fe(III), Fe-ammox can be responsible for substantial production of gaseous nitrogen species, such as N_2, N_2O or NO, and thus contribute to nitrogen loss and greenhouse gas emissions[172].

Balancing iron oxidation and reduction

Previous sections detailed the myriad of processes that make up the biogeochemical iron cycle. However, these processes are not separated in natural environments, where oxidation and reduction reactions occur cyclically or even simultaneously. For example, during redox cycling of a tropical forest soil, the iron(III) (oxyhydr)oxides formed during oxic periods became progressively less crystalline across repeated redox cycles, which facilitated even more rapid Fe(III) reduction with every reducing cycle[173]. Oxidative cycles need not only be initiated by oxygen but can also be promoted by nitrate under anoxic conditions[174].

Iron redox cycling does not always lead to mineral phase transformation, (for example, from ferrihydrite to siderite) but can occur within a single mineral phase. For instance, some mixed-valence iron minerals (that is, containing Fe(II) and Fe(III)) such as magnetite can function as both electron donors and electron acceptors, and therefore function as recyclable 'biogeobatteries' without transformation[5]. This process is size dependent, with oxidation confined to the surface and reduction enabling bulk electron transfer through the entire mineral[5].

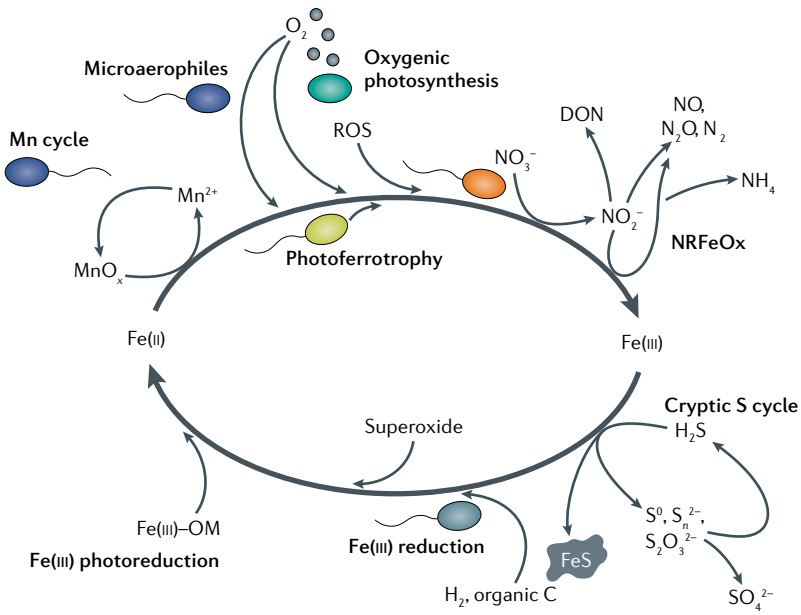

Fig. 4 | **Overview of processes that can overlap and lead to cryptic iron cycling.** Fe(II) is oxidized abiotically by molecular oxygen (O_2) formed during oxygenic photosynthesis, by reactive oxygen species (ROS) or by MnO_x formed during microbial Mn^{2+} oxidation (manganese cycle). Fe(II) is microbially oxidized either by phototrophic or microaerophilic Fe(II)-oxidizing bacteria. Fe(II) can also be microbially oxidized by nitrate (NRFeOx) and form nitrite, which abiotically oxidizes Fe(II), is further transformed via denitrification (producing NO, N_2O or N_2) or can transform to ammonium or dissolved organic nitrogen (DON). Fe(III) can be rapidly re-reduced by Fe(III)-reducing bacteria, by Fe(III) photoreduction, especially if Fe(III) is organically complexed (Fe(III)–organic matter (OM)), by superoxide or by sulfide (H_2S), leading either to precipitation of FeS minerals or to the formation of intermediate sulfur species (S^0, S_n^{2-} and $S_2O_3^{2-}$) that themselves are converted back to sulfide or to sulfate (SO_4^{2-}) (cryptic sulfur cycle).

Given the diversity of reactions that can cycle iron in the environment, it is not uncommon that they can spatially overlap[175]. In these cases, a cryptic cycling scenario can emerge in which turnover is so rapid that the product of iron oxidation or reduction cannot be measured with standard analytical techniques (FIG. 4). This cryptic cycling was observed in Lake Cadagno, Switzerland, where the re-reduction of Fe(III) in the stratified water column was so rapid that it masked the contribution of a population of Fe(II)-oxidizing bacteria[6]. A similar process was observed in laboratory incubations, when the activity of Fe(II)-oxidizing phototrophic bacteria was masked by the light-induced reduction of Fe(III) in iron–organic matter complexes[92]. This cryptic iron cycle may also be closely tied to the even more enigmatic processes in the sulfur cycle, with sulfate reduction hypothesized to drive Fe(III) reduction even when sulfide concentrations remain low[176]. The interactions between iron and nitrogen are also prime candidates for potential cryptic interactions in the iron cycle as the reactive nitrogen species produced are highly reactive and short-lived, and are thus unlikely to be accurately reflected in standard aqueous geochemical measurements. For example, in microbial nitrate-dependent Fe(III) oxidation by *Acidovorax* sp. BoFeN1, Fe(II) is not oxidized directly by the microorganisms but is oxidized by short-lived denitrification intermediates such as NO_2^- and NO[177]. These react so quickly with Fe(II) that they may never accumulate in solution despite contributing substantially to Fe(II) oxidation. Rapid reactions between iron and nitrogen species can promote incorporation of inorganic nitrogen into organic nitrogen, fundamentally altering soil nitrogen pools[178].

Conclusions

Since the discovery of the first iron-metabolizing bacteria, we have come a long way in our understanding of the diversity, physiology, ecology and environmental influence of the microorganisms that transform iron — and iron biogeochemistry remains a fascinating and complex subject of study. We are only just beginning to appreciate the complexity of iron transformations in the environment, and are increasingly adopting new tools (BOX 2) that will enable us in future research to observe and unravel the competing and co-occurring iron cycling processes. It has also become obvious that iron biogeochemical cycling is linked to future changes in Earth's climate via CO_2 formation and/or CH_4 oxidation by Fe(III)-reducing bacteria[9,122], CO_2 fixation by autotrophic Fe(II)-oxidizing bacteria[56] and N_2O formation by bacteria linking the iron and nitrogen cycles[102]. Further indirect effects on climate by iron-metabolizing bacteria are caused by iron mineral-precipitating and iron mineral-dissolving microorganisms that lead to mobilization or stabilization of organic carbon or nutrients[51,179,180], as well as by microorganisms that are involved in changing the bioavailability of iron species in the oceans, thus influencing primary productivity[76]. This leads us into an exciting new decade of iron biogeochemistry and opens up various future research directions.

Published online 1 February 2021

1. Ehrenberg, C. Vorläufige Mitteilungen über das wirkliche Vorkommen fossiler Infusorien und ihre große Verbreitung. *Poggendorff Ann.* **38**, 213–227 (1836).
2. Chan, C. S. et al. The architecture of iron microbial mats reflects the adaptation of chemolithotrophic iron oxidation in freshwater and marine environments. *Front. Microbiol.* https://doi.org/10.3389/fmicb.2016.00796 (2016).
Microscopic analysis indicates how the morphology of iron-oxidizing bacteria in microbial mats responds to environmental conditions.
3. Melton, E. D., Swanner, E. D., Behrens, S., Schmidt, C. & Kappler, A. The interplay of microbially mediated and abiotic reactions in the biogeochemical Fe cycle. *Nat. Rev. Microbiol.* **12**, 797–808 (2014).
4. Ehrlich, H. L., Newman, D. K. & Kappler, A. *Ehrlich's Geomicrobiology*. (CRC Press, 2015).
5. Byrne, J. M. et al. Redox cycling of Fe(II) and Fe(III) in magnetite by Fe-metabolizing bacteria. *Science* **347**, 1473–1476 (2015).
First article to demonstrate magnetite could support complete microbial iron cycling; that is, Fe(II) in magnetite can be used as an electron source by Fe(II) oxidizers and Fe(III) can be used by Fe(III) reducers as an electron acceptor in a cycling fashion.
6. Berg, J. S. et al. Intensive cryptic microbial iron cycling in the low iron water column of the meromictic Lake Cadagno. *Environ. Microbiol.* **18**, 5288–5302 (2016).
7. Kappler, A. & Bryce, C. Cryptic biogeochemical cycles: unravelling hidden redox reactions. *Environ. Microbiol.* **19**, 842–846 (2017).
8. Wang, M., Hu, R., Zhao, J., Kuzyakov, Y. & Liu, S. Iron oxidation affects nitrous oxide emissions via donating electrons to denitrification in paddy soils. *Geoderma* **271**, 173–180 (2016).
9. Beal, E. J., House, C. H. & Orphan, V. J. Manganese- and iron-dependent marine methane oxidation. *Science* **325**, 184–187 (2009).
First demonstration that methane oxidation can be coupled to reduction of iron(III) oxides and manganese(IV) oxides.
10. Orihel, D. M. et al. The "nutrient pump:" iron-poor sediments fuel low nitrogen-to-phosphorus ratios and cyanobacterial blooms in polymictic lakes. *Limnol. Oceanogr.* **60**, 856–871 (2015).
11. Lalonde, K., Mucci, A., Ouellet, A. & Gélinas, Y. Preservation of organic matter in sediments promoted by iron. *Nature* **483**, 198–200 (2012).
12. Muehe, E. M. et al. Fate of Cd during microbial Fe(III) mineral reduction by a novel and Cd-tolerant *Geobacter* species. *Environ. Sci. Technol.* **47**, 14099–14109 (2013).
13. Glodowska, M. et al. Role of in situ natural organic matter in mobilizing As during microbial reduction of Fe^{III}-mineral-bearing aquifer sediments from Hanoi (Vietnam). *Environ. Sci. Technol.* **54**, 4149–4159 (2020).
14. Cutting, R. S., Coker, V. S., Fellowes, J. W., Lloyd, J. R. & Vaughan, D. J. Mineralogical and morphological constraints on the reduction of Fe(III) minerals by *Geobacter sulfurreducens*. *Geochim. Cosmochim. Acta* **73**, 4004–4022 (2009).
15. Wu, T. et al. Interactions between Fe(III)-oxides and Fe(III)-phyllosilicates during microbial reduction 2: natural subsurface sediments. *Geomicrobiol. J.* **34**, 231–241 (2017).
16. Jaisi, D. P., Dong, H. & Liu, C. Influence of biogenic Fe(II) on the extent of microbial reduction of Fe(III) in clay minerals nontronite, illite, and chlorite. *Geochim. Cosmochim. Acta* **71**, 1145–1158 (2007).
17. Bosch, J., Heister, K., Hofmann, T. & Meckenstock, R. U. Nanosized iron oxide colloids strongly enhance microbial iron reduction. *Appl. Environ. Microbiol.* **76**, 184–189 (2010).
18. Aeppli, M. et al. Decreases in iron oxide reducibility during microbial reductive dissolution and transformation of ferrihydrite. *Environ. Sci. Technol.* **53**, 8736–8746 (2019).
19. Levar, C. E., Hoffman, C. L., Dunshee, A. J., Toner, B. M. & Bond, D. R. Redox potential as a master variable controlling pathways of metal reduction by *Geobacter sulfurreducens*. *ISME J.* **11**, 741–752 (2017).
20. Wang, Z. et al. Kinetics of reduction of Fe(III) complexes by outer membrane cytochromes MtrC and OmcA of *Shewanella oneidensis* MR-1. *Appl. Environ. Microbiol.* **74**, 6746–6755 (2008).
21. Kügler, S. et al. Iron-organic matter complexes accelerate microbial iron cycling in an iron-rich Fen. *Sci. Total. Environ.* **646**, 972–988 (2019).
22. Daugherty, E. E., Gilbert, B., Nico, P. S. & Borch, T. Complexation and redox buffering of iron(II) by dissolved organic matter. *Environ. Sci. Technol.* **51**, 11096–11104 (2017).
23. von der Heyden, B., Roychoudhury, A. & Myneni, S. Iron-rich nanoparticles in natural aquatic environments. *Minerals* **9**, 287 (2019).
Thorough review of the nature and impact of iron nanoparticles in the environment.
24. Hassellöv, M. & von der Kammer, F. Iron oxides as geochemical nanovectors for metal transport in soil-river systems. *Elements* **4**, 401–406 (2008).
25. Liu, J. et al. Particle size effect and the mechanism of hematite reduction by the outer membrane cytochrome OmcA of *Shewanella oneidensis* MR-1. *Geochim. Cosmochim. Acta* **193**, 160–175 (2016).
26. Druschel, G. K., Emerson, D., Sutka, R., Suchecki, P. & Luther, G. W. Low-oxygen and chemical kinetic constraints on the geochemical niche of neutrophilic iron(II) oxidizing microorganisms. *Geochim. Cosmochim. Acta* **72**, 3358–3370 (2008).
Landmark study using voltammetric electrodes to elucidate the optimum geochemical conditions of microaerophilic Fe(II) oxidizers.
27. Barnes, A., Sapsford, D. J., Dey, M. & Williams, K. P. Heterogeneous Fe(II) oxidation and zeta potential. *J. Geochem. Explor.* **100**, 192–198 (2009).
28. González-Davila, M., Santana-Casiano, J. M. & Millero, F. J. Oxidation of iron (II) nanomolar with H_2O_2 in seawater. *Geochim. Cosmochim. Acta* **69**, 83–93 (2005).
29. Kanzaki, Y. & Murakami, T. Rate law of Fe(II) oxidation under low O_2 conditions. *Geochim. Cosmochim. Acta* **123**, 338–350 (2013).
30. King, D. W., Lounsbury, H. A. & Millero, F. J. Rates and mechanism of Fe(II) oxidation at nanomolar total iron concentrations. *Environ. Sci. Technol.* **29**, 818–824 (1995).
31. Emerson, D., Fleming, E. J. & McBeth, J. M. Iron-oxidizing bacteria: an environmental and genomic perspective. *Annu. Rev. Microbiol.* **64**, 561–583 (2010).
32. Chan, C. S., Emerson, D. & Luther, G. W. III The role of microaerophilic Fe-oxidizing micro-organisms in producing banded iron formations. *Geobiology* **14**, 509–528 (2016).
33. Mori, J. F. et al. Physiological and ecological implications of an iron- or hydrogen-oxidizing member of the Zetaproteobacteria, *Ghiorsea bivora*, gen. nov., sp. nov. *ISME J.* **11**, 2624–2636 (2017).
34. Emerson, D. & De Vet, W. The role of FeOB in engineered water ecosystems: a review. *J. AWWA* **107**, E47–E57 (2015).
35. MacDonald, D. J. et al. Using in situ voltammetry as a tool to identify and characterize habitats of iron-oxidizing bacteria: from fresh water wetlands to hydrothermal vent sites. *Environ. Sci. Process. Impacts* **16**, 2117–2126 (2014).
36. Emerson, D., Weiss, J. V. & Megonigal, J. P. Iron-oxidizing bacteria are associated with ferric hydroxide precipitates (Fe-plaque) on the roots of wetland plants. *Appl. Environ. Microbiol.* **65**, 2758–2761 (1999).
37. Laufer, K. et al. Microaerophilic Fe(II)-oxidizing *Zetaproteobacteria* isolated from low-Fe marine coastal sediments: physiology and composition of their twisted stalks. *Appl. Environ. Microbiol.* **83**, e03118–03116 (2017).
38. Orcutt, B. N. et al. Colonization of subsurface microbial observatories deployed in young ocean crust. *ISME J.* **5**, 692–703 (2011).
39. Field, E. K. et al. Planktonic marine iron oxidizers drive iron mineralization under low-oxygen conditions. *Geobiology* **14**, 499–508 (2016).
40. Maisch, M. et al. Contribution of microaerophilic iron(II)-oxidizers to iron(III) mineral formation. *Environ. Sci. Technol.* **53**, 8197–8204 (2019).
41. Chiu, B. K., Kato, S., McAllister, S. M., Field, E. K. & Chan, C. S. Novel pelagic iron-oxidizing Zetaproteobacteria from the Chesapeake Bay oxic–anoxic transition zone. *Front. Microbiol.* **8**, 1280 (2017).
42. McAllister, S. M. et al. The Fe(II)-oxidizing *Zetaproteobacteria*: historical, ecological and genomic perspectives. *FEMS Microbiol. Ecol.* https://doi.org/10.1093/femsec/fiz015 (2019).
43. Barco, R. A. et al. New insight into microbial iron oxidation as revealed by the proteomic profile of an obligate iron-oxidizing chemolithoautotroph. *Appl. Environ. Microbiol.* **81**, 5927–5937 (2015).
44. McAllister, S. M. et al. Validating the Cyc2 neutrophilic iron oxidation pathway using meta-omics of *Zetaproteobacteria* iron mats at marine hydrothermal vents. *mSystems* **5**, e00553–00519 (2020).
Support for Cyc2 as the iron oxidase in microaerophilic Fe(II) oxidizers.
45. Jeans, C. et al. Cytochrome 572 is a conspicuous membrane protein with iron oxidation activity purified directly from a natural acidophilic microbial community. *ISME J.* **2**, 542–550 (2008).
46. Edwards, B. A. & Ferris, F. G. Influence of water flow on in situ rates of bacterial Fe(II) oxidation. *Geomicrobiol. J.* **37**, 67–75 (2020).
47. Liu, J. et al. Identification and characterization of MtoA: a decaheme c-type cytochrome of the neutrophilic Fe(II)-oxidizing bacterium *Sideroxydans lithotrophicus* ES-1. *Front. Microbiol.* **3**, 37 (2012).
48. Chan, C. S., McAllister, S. M., Garber, A., Hallahan, B. J. & Rozovsky, S. Fe oxidation by a fused cytochrome-porin common to diverse Fe-oxidizing bacteria. *bioRxiv* https://doi.org/10.1101/228056 (2018).
49. Byrne, J. M., Schmidt, M., Gauger, T., Bryce, C. & Kappler, A. Imaging organic–mineral aggregates formed by Fe(II)-oxidizing bacteria using helium ion microscopy. *Environ. Sci. Technol. Lett.* **5**, 209–213 (2018).
50. Krepski, S. T., Emerson, D., Hredzak-Showalter, P. L., Luther, G. W. III & Chan, C. S. Morphology of biogenic iron oxides records microbial physiology and environmental conditions: toward interpreting iron microfossils. *Geobiology* **11**, 457–471 (2013).
51. Sowers, T. D., Holden, K. L., Coward, E. K. & Sparks, D. L. Dissolved organic matter sorption and molecular fractionation by naturally occurring bacteriogenic iron (oxyhydr)oxides. *Environ. Sci. Technol.* **53**, 4295–4304 (2019).
52. Lueder, U., Druschel, G., Emerson, D., Kappler, A. & Schmidt, C. Quantitative analysis of O_2 and Fe^{2+} profiles in gradient tubes for cultivation of microaerophilic iron(II)-oxidizing bacteria. *FEMS Microbiol. Ecol.* https://doi.org/10.1093/femsec/fix177 (2017).
53. van der Grift, B., Rozemeijer, J. C., Griffioen, J. & van der Velde, Y. Iron oxidation kinetics and phosphate immobilization along the flow-path from groundwater into surface water. *Hydrol. Earth Syst. Sci.* **18**, 4687–4702 (2014).
54. Enright, A. M. L. & Ferris, F. G. Bacterial Fe(II) oxidation distinguished by long-range correlation in redox potential. *J. Geophys. Res. Biogeosci.* **121**, 1249–1257 (2016).
55. Lueder, U., Jørgensen, B. B., Kappler, A. & Schmidt, C. Photochemistry of iron in aquatic environments. *Environ. Sci. Process. Impacts* **22**, 12–24 (2020).
56. Widdel, F. et al. Ferrous iron oxidation by anoxygenic phototrophic bacteria. *Nature* **362**, 834–836 (1993).
57. Hartman, H. *The Evolution of Photosynthesis and Microbial Mats: A Speculation on the Banded Iron Formations*. (Alan R. Liss, Inc., 1984).
58. Ozaki, K., Tajika, E., Hong, P. K., Nakagawa, Y. & Reinhard, C. T. Effects of primitive photosynthesis on Earth's early climate system. *Nat. Geosci.* **11**, 55–59 (2018).
59. Croal, L. R., Jiao, Y. & Newman, D. K. The *fox* operon from *Rhodobacter* strain SW2 promotes phototrophic Fe(II) oxidation in *Rhodobacter capsulatus* SB1003. *J. Bacteriol.* **189**, 1774–1782 (2007).
60. Ehrenreich, A. & Widdel, F. Anaerobic oxidation of ferrous iron by purple bacteria, a new type of phototrophic metabolism. *Appl. Environ. Microbiol.* **60**, 4517–4526 (1994).
61. Jiao, Y., Kappler, A., Croal, L. R. & Newman, D. K. Isolation and characterization of a genetically tractable photoautotrophic Fe(II)-oxidizing bacterium, *Rhodopseudomonas palustris* strain TIE-1. *Appl. Environ. Microbiol.* **71**, 4487–4496 (2005).
62. Straub, K. L., Rainey, F. A. & Widdel, F. *Rhodovulum iodosum* sp. nov. and *Rhodovulum robiginosum* sp. nov., two new marine phototrophic ferrous-iron-oxidizing purple bacteria. *Int. J. Syst. Evol. Microbiol.* **49**, 729–735 (1999).
63. Heising, S., Richter, L., Ludwig, W. & Schink, B. *Chlorobium ferrooxidans* sp. nov., a phototrophic green sulfur bacterium that oxidizes ferrous iron in coculture with a *Geospirillum* sp. strain. *Arch. Microbiol.* **172**, 116–124 (1999).
64. Llirós, M. et al. Pelagic photoferrotrophy and iron cycling in a modern ferruginous basin. *Sci. Rep.* **5**, 13803 (2015).
65. Laufer, K. et al. Physiological characterization of a halotolerant anoxygenic phototrophic Fe(II)-oxidizing green-sulfur bacterium isolated from a marine sediment. *FEMS Microbiol. Ecol.* https://doi.org/10.1093/femsec/fix054 (2017).

66. Jiao, Y. & Newman, D. K. The *pio* operon is essential for phototrophic Fe(II) oxidation in *Rhodopseudomonas palustris* TIE-1. *J. Bacteriol.* **189**, 1765–1773 (2007).
67. Gupta, D. et al. Photoferrotrophs produce a PioAB electron conduit for extracellular electron uptake. *mBio* **10**, e02668–02619 (2019).
68. Gledhill, M. & Buck, K. The organic complexation of iron in the marine environment: A review. *Front. Microbiol.* **3**, 69 (2012).
69. Saraiva, I. H., Newman, D. K. & Louro, R. O. Functional characterization of the FoxE iron oxidoreductase from the photoferrotroph *Rhodobacter ferrooxidans* SW2. *J. Biol. Chem.* **287**, 25541–25548 (2012).
70. Crowe, S. A. et al. Draft genome sequence of the pelagic photoferrotroph *Chlorobium phaeoferrooxidans*. *Genome Announc.* **5**, e01584–01516 (2017).
71. Bryce, C., Blackwell, N., Straub, D., Kleindienst, S. & Kappler, A. Draft genome sequence of *Chlorobium* sp. strain N1, a marine Fe(II)-oxidizing green sulfur bacterium. *Microbiol. Resour. Announc.* **8**, e00080–00019 (2019).
72. Miot, J. et al. Iron biomineralization by anaerobic neutrophilic iron-oxidizing bacteria. *Geochim. Cosmochim. Acta* **73**, 696–711 (2009).
73. Schaedler, S. et al. Formation of cell-iron-mineral aggregates by phototrophic and nitrate-reducing anaerobic Fe(II)-oxidizing bacteria. *Geomicrobiol. J.* **26**, 93–103 (2009).
74. Hegler, F., Schmidt, C., Schwarz, H. & Kappler, A. Does a low-pH microenvironment around phototrophic Fe^{II}-oxidizing bacteria prevent cell encrustation by Fe^{III} minerals? *FEMS Microbiol. Ecol.* **74**, 592–600 (2010).
75. Swanner, E. D. et al. Fractionation of Fe isotopes during Fe(II) oxidation by a marine photoferrotroph is controlled by the formation of organic Fe-complexes and colloidal Fe fractions. *Geochim. Cosmochim. Acta* **165**, 44–61 (2015).
76. Boyd, P. W. & Ellwood, M. J. The biogeochemical cycle of iron in the ocean. *Nat. Geosci.* **3**, 675–682 (2010). **A comprehensive review of the many dynamic processes which influence iron cycling in the oceans**.
77. Faust, B. C. & Zepp, R. G. Photochemistry of aqueous iron(III)-polycarboxylate complexes: roles in the chemistry of atmospheric and surface waters. *Environ. Sci. Technol.* **27**, 2517–2522 (1993).
78. Rose, A. L. & Waite, T. D. Reduction of organically complexed ferric iron by superoxide in a simulated natural water. *Environ. Sci. Technol.* **39**, 2645–2650 (2005).
79. Voelker, B. M., Morel, F. M. M. & Sulzberger, B. Iron redox cycling in surface waters: Effects of humic substances and light. *Environ. Sci. Technol.* **31**, 1004–1011 (1997).
80. Barbeau, K., Zhang, G., Live, D. H. & Butler, A. Petrobactin, a photoreactive siderophore produced by the oil-degrading marine bacterium *Marinobacter hydrocarbonoclasticus*. *J. Am. Chem. Soc.* **124**, 378–379 (2002).
81. Waite, T. D. & Morel, F. M. M. Photoreductive dissolution of colloidal iron oxides in natural waters. *Environ. Sci. Technol.* **18**, 860–868 (1984).
82. Sulzberger, B. Light-induced redox cycling of iron: roles for CO_2 uptake and release by aquatic ecosystems. *Aquat. Geochem.* **21**, 65–80 (2015).
83. Garg, S., Rose, A. L. & Waite, T. D. Photochemical production of superoxide and hydrogen peroxide from natural organic matter. *Geochim. Cosmochim. Acta* **75**, 4310–4320 (2011).
84. Xing, G., Garg, S. & Waite, T. D. Is superoxide-mediated Fe(III) reduction important in sunlit surface waters? *Environ. Sci. Technol.* **53**, 13179–13190 (2019).
85. Sutherland, K. M., Wankel, S. D. & Hansel, C. M. Dark biological superoxide production as a significant flux and sink of marine dissolved oxygen. *Proc. Natl. Acad. Sci. USA* **117**, 3433–3439 (2020).
86. Diaz, J. M. et al. Widespread production of extracellular superoxide by heterotrophic bacteria. *Science* **340**, 1223–1226 (2013).
87. Lis, H., Kranzler, C., Keren, N. & Shaked, Y. A comparative study of iron uptake rates and mechanisms amongst marine and fresh water cyanobacteria: prevalence of reductive iron uptake. *Life* **5**, 841–860 (2015).
88. Swanner, E. D., Maisch, M., Wu, W. & Kappler, A. Oxic Fe(III) reduction could have generated Fe(II) in the photic zone of Precambrian seawater. *Sci. Rep.* **8**, 4238 (2018).
89. Emmenegger, L., Schönenberger, R., Sigg, L. & Sulzberger, B. Light-induced redox cycling of iron in circumneutral lakes. *Limnol. Oceanogr.* **46**, 49–61 (2001).
90. Lueder, U., Jørgensen, B. B., Kappler, A. & Schmidt, C. Fe(III) photoreduction producing Fe_{aq}^{2+} in oxic freshwater sediment. *Environ. Sci. Technol.* **54**, 862–869 (2020).
91. Lueder, U. et al. Influence of physical perturbation on Fe(II) supply in coastal marine sediments. *Environ. Sci. Technol.* **54**, 3209–3218 (2020).
92. Peng, C., Bryce, C., Sundman, A. & Kappler, A. Cryptic cycling of complexes containing Fe(III) and organic matter by phototrophic Fe(II)-oxidizing bacteria. *Appl. Environ. Microbiol.* **85**, e02826–02818 (2019).
93. Schmidt, C., Behrens, S. & Kappler, A. Ecosystem functioning from a geomicrobiological perspective a conceptual framework for biogeochemical iron cycling. *Environ. Chem.* **7**, 399–405 (2010).
94. Raven, J. A., Kübler, J. E. & Beardall, J. Put out the light, and then put out the light. *J. Mar. Biol. Assoc. U.K.* **80**, 1–25 (2000).
95. Camacho, A., Walter, X. A., Picazo, A. & Zopfi, J. Photoferrotrophy: Remains of an ancient photosynthesis in modern environments. *Front. Microbiol.* **8** (2017). **A review on the physiology of anoxygenic phototrophic Fe(II) oxidizers and their role in modern and ancient redox-stratified systems**.
96. Crowe, S. A. et al. Deep-water anoxygenic photosythesis in a ferruginous chemocline. *Geobiology* **12**, 322–339 (2014).
97. Straub, K. L., Benz, M., Schink, B. & Widdel, F. Anaerobic, nitrate-dependent microbial oxidation of ferrous iron. *Appl. Environ. Microbiol.* **62**, 1458–1460 (1996).
98. Bryce, C. et al. Microbial anaerobic Fe(II) oxidation – Ecology, mechanisms and environmental implications. *Environ. Microbiol.* **20**, 3462–3483 (2018).
99. Blöthe, M. & Roden, E. E. Composition and activity of an autotrophic Fe(II)-oxidizing, nitrate-reducing enrichment culture. *Appl. Environ. Microbiol.* **75**, 6937–6940 (2009). **Article describing the composition of the only confirmed autotrophic nitrate-dependent, Fe(II)-oxidizing enrichment culture**.
100. Laufer, K., Røy, H., Jørgensen, B. B. & Kappler, A. Evidence for the existence of autotrophic nitrate-reducing Fe(II)-oxidizing bacteria in marine coastal sediment. *Appl. Environ. Microbiol.* **82**, 6120–6131 (2016).
101. Liu, T., Chen, D., Luo, X., Li, X. & Li, F. Microbially mediated nitrate-reducing Fe(II) oxidation: quantification of chemodenitrification and biological reactions. *Geochim. Cosmochim. Acta* **256**, 97–115 (2019).
102. Otte, J. M. et al. N_2O formation by nitrite-induced (chemo)denitrification in coastal marine sediment. *Sci. Rep.* **9**, 10691 (2019).
103. Wang, M., Hu, R., Ruser, R., Schmidt, C. & Kappler, A. Role of chemodenitrification for N_2O emissions from nitrate reduction in rice paddy soils. *ACS Earth Space Chem.* **4**, 122–132 (2020).
104. He, S., Tominski, C., Kappler, A., Behrens, S. & Roden, E. E. Metagenomic analyses of the autotrophic Fe(II)-oxidizing, nitrate-reducing enrichment culture KS. *Appl. Environ. Microbiol.* **82**, 2656–2668 (2016).
105. Buchwald, C., Grabb, K., Hansel, C. M. & Wankel, S. D. Constraining the role of iron in environmental nitrogen transformations: Dual stable isotope systematics of abiotic NO_2^- reduction by Fe(II) and its production of N_2O. *Geochim. Cosmochim. Acta* **186**, 1–12 (2016).
106. Haaijer, S. C. M., Lamers, L. P. M., Smolders, A. J. P., Jetten, M. S. M. & Op den Camp, H. J. M. Iron sulfide and pyrite as potential electron donors for microbial nitrate reduction in freshwater wetlands. *Geomicrobiol. J.* **24**, 391–401 (2007).
107. Edwards, K. J., Rogers, D. R., Wirsen, C. O. & McCollom, T. M. Isolation and characterization of novel psychrophilic, neutrophilic, Fe-oxidizing, chemolithoautotrophic α- and γ-*Proteobacteria* from the deep sea. *Appl. Environ. Microbiol.* **69**, 2906–2913 (2003).
108. Yan, R. et al. Effect of reduced sulfur species on chemolithoautotrophic pyrite oxidation with nitrate. *Geomicrobiol. J.* **36**, 19–29 (2019).
109. Holmes, P. R. & Crundwell, F. K. The kinetics of the oxidation of pyrite by ferric ions and dissolved oxygen: an electrochemical study. *Geochim. Cosmochim. Acta* **64**, 263–274 (2000).
110. Zhao, L., Dong, H., Edelmann, R. E., Zeng, Q. & Agrawal, A. Coupling of Fe(II) oxidation in illite with nitrate reduction and its role in clay mineral transformation. *Geochim. Cosmochim. Acta* **200**, 353–366 (2017).
111. Zhang, L., Dong, H., Kukkadapu, R. K., Jin, Q. & Kovarik, L. Electron transfer between sorbed Fe(II) and structural Fe(III) in smectites and its effect on nitrate-dependent iron oxidation by *Pseudogulbenkiania* sp. strain 2002. *Geochim. Cosmochim. Acta* **265**, 132–147 (2019).
112. Shelobolina, E. S., VanPraagh, C. G. & Lovley, D. R. Use of ferric and ferrous iron containing minerals for respiration by *Desulfitobacterium frappieri*. *Geomicrobiol. J.* **20**, 143–156 (2003).
113. Larese-Casanova, P., Haderlein, S. B. & Kappler, A. Biomineralization of lepidocrocite and goethite by nitrate-reducing Fe(II)-oxidizing bacteria: effect of pH, bicarbonate, phosphate, and humic acids. *Geochim. Cosmochim. Acta* **74**, 3721–3734 (2010).
114. Pantke, C. et al. Green rust formation during Fe(II) oxidation by the nitrate-reducing *Acidovorax* sp. strain BoFeN1. *Environ. Sci. Technol.* **46**, 1439–1446 (2012).
115. Nordhoff, M. et al. Insights into nitrate-reducing Fe(II) oxidation mechanisms through analysis of cell-mineral associations, cell encrustation, and mineralogy in the chemolithoautotrophic enrichment culture KS. *Appl. Environ. Microbiol.* **83**, e00752–00717 (2017).
116. Smith, R. L., Kent, D. B., Repert, D. A. & Böhlke, J. K. Anoxic nitrate reduction coupled with iron oxidation and attenuation of dissolved arsenic and phosphate in a sand and gravel aquifer. *Geochim. Cosmochim. Acta* **196**, 102–120 (2017).
117. Madison, A. S., Tebo, B. M., Mucci, A., Sundby, B. & Luther, G. W. Abundant porewater Mn(III) is a major component of the sedimentary redox system. *Science* **341**, 875–878 (2013).
118. Gillispie, E. C., Taylor, S. E., Qafoku, N. P. & Hochella, M. F. Jr. Impact of iron and manganese nano-metal-oxides on contaminant interaction and fortification potential in agricultural systems – a review. *Environ. Chem.* **16**, 377–390 (2019).
119. Siebecker, M., Madison, A. S. & Luther, G. W. Reduction kinetics of polymeric (soluble) manganese (IV) oxide (MnO_2) by ferrous iron (Fe^{2+}). *Aquat. Geochem.* **21**, 143–158 (2015).
120. Herndon, E. M., Havig, J. R., Singer, D. M., McCormick, M. L. & Kump, L. R. Manganese and iron geochemistry in sediments underlying the redox-stratified Fayetteville Green Lake. *Geochim. Cosmochim. Acta* **231**, 50–63 (2018).
121. Maguffin, S. C. et al. Influence of manganese abundances on iron and arsenic solubility in rice paddy soils. *Geochim. Cosmochim. Acta* **276**, 50–69 (2020).
122. Lovley, D. R. & Phillips, E. J. P. Novel mode of microbial energy metabolism: Organic carbon oxidation coupled to dissimilatory reduction of iron or manganese. *Appl. Environ. Microbiol.* **54**, 1472–1480 (1988).
123. Myers, C. R. & Nealson, K. H. Respiration-linked proton translocation coupled to anaerobic reduction of manganese(IV) and iron(III) in *Shewanella putrefaciens* MR-1. *J. Bacteriol.* **172**, 6232–6238 (1990).
124. Lovley, D. R., Coates, J. D., Blunt-Harris, E. L., Phillips, E. J. P. & Woodward, J. C. Humic substances as electron acceptors for microbial respiration. *Nature* **382**, 445–448 (1996).
125. Coates, J. D., Ellis, D. J., Gaw, C. V. & Lovley, D. R. *Geothrix fermentans* gen. nov., sp. nov., a novel Fe(III)-reducing bacterium from a hydrocarbon-contaminated aquifer. *Int. J. Syst. Evol. Microbiol.* **49**, 1615–1622 (1999).
126. Tor, J. M. & Lovley, D. R. Anaerobic degradation of aromatic compounds coupled to Fe(III) reduction by *Ferroglobus placidus*. *Environ. Microbiol.* **3**, 281–287 (2001).
127. Hansel, C. M., Benner, S. G. & Fendorf, S. Competing Fe(II)-induced mineralization pathways of ferrihydrite. *Environ. Sci. Technol.* **39**, 7147–7153 (2005).
128. Shi, L. et al. The roles of outer membrane cytochromes of *Shewanella* and *Geobacter* in extracellular electron transfer. *Environ. Microbiol. Rep.* **1**, 220–227 (2009).
129. Shi, L., Squier, T. C., Zachara, J. M. & Fredrickson, J. K. Respiration of metal (hydr)oxides by *Shewanella* and *Geobacter*: a key role for multihaem *c*-type cytochromes. *Mol. Microbiol.* **65**, 12–20 (2007).
130. Butler, J. E., Young, N. D. & Lovley, D. R. Evolution of electron transfer out of the cell: comparative genomics of six *Geobacter* genomes. *BMC Genomics* **11**, 40 (2010).

131. Reguera, G. et al. Biofilm and nanowire production leads to increased current in *Geobacter sulfurreducens* fuel cells. *Appl. Environ. Microbiol.* **72**, 7345–7348 (2006).
132. Lovley, D. R. & Holmes, D. E. Protein nanowires: the electrification of the microbial world and maybe our own. *J. Bacteriol.* **202**, e00331–00320 (2020). **A comprehensive and recent review on extracellular electron transfer by bacteria**.
133. Reguera, G. et al. Extracellular electron transfer via microbial nanowires. *Nature* **435**, 1098–1101 (2005).
134. Cologgi, D. L., Lampa-Pastirk, S., Speers, A. M., Kelly, S. D. & Reguera, G. Extracellular reduction of uranium via *Geobacter* conductive pili as a protective cellular mechanism. *Proc. Natl. Acad. Sci. USA* **108**, 15248–15252 (2011).
135. Ueki, T. et al. Decorating the outer surface of microbially produced protein nanowires with peptides. *ACS Synth. Biol.* **8**, 1809–1817 (2019).
136. Smith, J. A., Lovley, D. R. & Tremblay, P.-L. Outer cell surface components essential for Fe(III) oxide reduction by *Geobacter metallireducens*. *Appl. Environ. Microbiol.* **79**, 901–907 (2013).
137. Pirbadian, S. et al. *Shewanella oneidensis* MR-1 nanowires are outer membrane and periplasmic extensions of the extracellular electron transport components. *Proc. Natl. Acad. Sci. USA* **111**, 12883–12888 (2014).
138. El-Naggar, M. Y. et al. Electrical transport along bacterial nanowires from *Shewanella oneidensis* MR-1. *Proc. Natl. Acad. Sci. USA* **107**, 18127–18131 (2010).
139. Roden, E. E. et al. Extracellular electron transfer through microbial reduction of solid-phase humic substances. *Nat. Geosci.* **3**, 417–421 (2010).
140. Lohmayer, R., Kappler, A., Lösekann-Behrens, T. & Planer-Friedrich, B. Sulfur species as redox partners and electron shuttles for ferrihydrite reduction by *Sulfurospirillum deleyianum*. *Appl. Environ. Microbiol.* **80**, 3141–3149 (2014).
141. Kappler, A., Benz, M., Schink, B. & Brune, A. Electron shuttling via humic acids in microbial iron(III) reduction in a freshwater sediment. *FEMS Microbiol. Ecol.* **47**, 85–92 (2004).
142. Cervantes, F. J. et al. Reduction of humic substances by halorespiring, sulphate-reducing and methanogenic microorganisms. *Environ. Microbiol.* **4**, 51–57 (2002).
143. Coates, J. D. et al. Recovery of humic-reducing bacteria from a diversity of environments. *Appl. Environ. Microbiol.* **64**, 1504–1509 (1998).
144. Piepenbrock, A., Behrens, S. & Kappler, A. Comparison of humic substance- and Fe(III)-reducing microbial communities in anoxic aquifers. *Geomicrobiol. J.* **31**, 917–928 (2014).
145. Canfield, D. E. Reactive iron in marine sediments. *Geochim. Cosmochim. Acta* **53**, 619–632 (1989).
146. Marsili, E. et al. *Shewanella* secretes flavins that mediate extracellular electron transfer. *Proc. Natl. Acad. Sci. USA* **105**, 3968–3973 (2008).
147. von Canstein, H., Ogawa, J., Shimizu, S. & Lloyd, J. R. Secretion of flavins by *Shewanella* species and their role in extracellular electron transfer. *Appl. Environ. Microbiol.* **74**, 615–623 (2008).
148. Nevin, K. P. & Lovley, D. R. Mechanisms for Fe(III) oxide reduction in sedimentary environments. *Geomicrobiol. J.* **19**, 141–159 (2002).
149. Markelova, E. et al. Deconstructing the redox cascade: what role do microbial exudates (flavins) play? *Environ. Chem.* **14**, 515–524 (2017).
150. Bai, Y. et al. AQDS and redox-active NOM enables microbial Fe(III)-mineral reduction at cm-scales. *Environ. Sci. Technol.* **54**, 4131–4139 (2020). **The first article to demonstrate that microorganisms can transfer electrons to Fe(III) over centimetre distances by electron shuttling**.
151. Bai, Y., Sun, T., Angenent, L. T., Haderlein, S. B. & Kappler, A. Electron hopping enables rapid electron transfer between quinone-/hydroquinone-containing organic molecules in microbial iron(III) mineral reduction. *Environ. Sci. Technol.* **54**, 10646–10653 (2020).
152. Liu, F. et al. Magnetite compensates for the lack of a pilin-associated c-type cytochrome in extracellular electron exchange. *Environ. Microbiol.* **17**, 648–655 (2015).
153. Taillefert, M. et al. *Shewanella putrefaciens* produces an Fe(III)-solubilizing organic ligand during anaerobic respiration on insoluble Fe(III) oxides. *J. Inorg. Biochem.* **101**, 1760–1767 (2007).
154. in 't Zandt, M. H., de Jong, A. E., Slomp, C. P. & Jetten, M. S. The hunt for the most-wanted chemolithoautotrophic spookmicrobes. *FEMS Microbiol. Ecol.* https://doi.org/10.1093/femsec/fiy064 (2018).
155. Sivan, O. et al. Geochemical evidence for iron-mediated anaerobic oxidation of methane. *Limnol. Oceanogr.* **56**, 1536–1544 (2011).
156. Miura, Y., Watanabe, A., Murase, J. & Kimura, M. Methane production and its fate in paddy fields. *Soil Sci. Plant Nutr.* **38**, 673–679 (1992).
157. Crowe, S. A. et al. The methane cycle in ferruginous Lake Matano. *Geobiology* **9**, 61–78 (2011).
158. Amos, R. T. et al. Evidence for iron-mediated anaerobic methane oxidation in a crude oil-contaminated aquifer. *Geobiology* **10**, 506–517 (2012).
159. Glodowska, M. et al. Arsenic mobilization by anaerobic iron-dependent methane oxidation. *Commun. Earth Environ.* **1**, 42 (2020). **First study providing evidence that anaerobic oxidation of methane coupled to reduction of arsenic-bearing Fe(III) minerals can lead to arsenic mobilization in groundwater**.
160. Scheller, S., Yu, H., Chadwick, G. L., McGlynn, S. E. & Orphan, V. J. Artificial electron acceptors decouple archaeal methane oxidation from sulfate reduction. *Science* **351**, 703–707 (2016).
161. Wegener, G., Krukenberg, V., Riedel, D., Tegetmeyer, H. E. & Boetius, A. Intercellular wiring enables electron transfer between methanotrophic archaea and bacteria. *Nature* **526**, 587–590 (2015).
162. Ettwig, K. F. et al. Archaea catalyze iron-dependent anaerobic oxidation of methane. *Proc. Natl. Acad. Sci. USA* **113**, 12792–12796 (2016).
163. Cai, C. et al. A methanotrophic archaeon couples anaerobic oxidation of methane to Fe(III) reduction. *ISME J.* **12**, 1929–1939 (2018).
164. Clément, J.-C., Shrestha, J., Ehrenfeld, J. G. & Jaffé, P. R. Ammonium oxidation coupled to dissimilatory reduction of iron under anaerobic conditions in wetland soils. *Soil. Biol. Biochem.* **37**, 2323–2328 (2005).
165. Huang, S. & Jaffé, P. R. Characterization of incubation experiments and development of an enrichment culture capable of ammonium oxidation under iron-reducing conditions. *Biogeosciences* **12**, 769–779 (2015).
166. Li, X. et al. Evidence of nitrogen loss from anaerobic ammonium oxidation coupled with ferric iron reduction in an intertidal wetland. *Environ. Sci. Technol.* **49**, 11560–11568 (2015).
167. Zhou, G.-W. et al. Electron shuttles enhance anaerobic ammonium oxidation coupled to iron(III) reduction. *Environ. Sci. Technol.* **50**, 9298–9307 (2016).
168. Yang, W. H., Weber, K. A. & Silver, W. L. Nitrogen loss from soil through anaerobic ammonium oxidation coupled to iron reduction. *Nat. Geosci.* **5**, 538–541 (2012).
169. Li, X. et al. Simultaneous Fe(III) reduction and ammonia oxidation process in Anammox sludge. *J. Environ. Sci.* **64**, 42–50 (2018).
170. Huang, S. & Jaffé, P. R. Isolation and characterization of an ammonium-oxidizing iron reducer: *Acidimicrobiaceae* sp. A6. *PLoS ONE* **13**, e0194007 (2018).
171. Sawayama, S. Possibility of anoxic ferric ammonium oxidation. *J. Biosci. Bioeng.* **101**, 70–72 (2006).
172. Zhu, X., Burger, M., Doane, T. A. & Horwath, W. R. Ammonia oxidation pathways and nitrifier denitrification are significant sources of N_2O and NO under low oxygen availability. *Proc. Natl. Acad. Sci. USA* **110**, 6328–6333 (2013).
173. Ginn, B., Meile, C., Wilmoth, J., Tang, Y. & Thompson, A. Rapid iron reduction rates are stimulated by high-amplitude redox fluctuations in a tropical forest soil. *Environ. Sci. Technol.* **51**, 3250–3259 (2017). **A good example of the dynamic nature of iron cycling in the environment and its impact on the reducibility of minerals**.
174. Mejia, J., Roden, E. E. & Ginder-Vogel, M. Influence of oxygen and nitrate on Fe (hydr)oxide mineral transformation and soil microbial communities during redox cycling. *Environ. Sci. Technol.* **50**, 3580–3588 (2016).
175. Laufer, K. et al. Coexistence of microaerophilic, nitrate-reducing, and phototrophic Fe(II) oxidizers and Fe(III) reducers in coastal marine sediment. *Appl. Environ. Microbiol.* **82**, 1433–1447 (2016).
176. Hansel, C. M., Ferdelman, T. G. & Tebo, B. M. Cryptic cross-linkages among biogeochemical cycles: novel insights from reactive intermediates. *Elements* **11**, 409–414 (2015). **A review on cryptic element cycling in the environment, including cryptic iron cycling**.
177. Klueglein, N. & Kappler, A. Abiotic oxidation of Fe(II) by reactive nitrogen species in cultures of the nitrate-reducing Fe(II) oxidizer *Acidovorax* sp. BoFeN1 – questioning the existence of enzymatic Fe(II) oxidation. *Geobiology* **11**, 180–190 (2013).
178. Matus, F. et al. Ferrous wheel hypothesis: Abiotic nitrate incorporation into dissolved organic matter. *Geochim. Cosmochim. Acta* **245**, 514–524 (2019). **Demonstration of the 'ferrous wheel hypothesis' with insights for the role of coupled iron and nitrogen cycling in the environment**.
179. Chen, C., Hall, S. J., Coward, E. & Thompson, A. Iron-mediated organic matter decomposition in humid soils can counteract protection. *Nat. Commun.* **11**, 2255 (2020).
180. Patzner, M. S. et al. Iron mineral dissolution releases iron and associated organic carbon during permafrost thaw. *Nat. Commun.* **11**, 6329 (2020).
181. Beckwith, C. R. et al. Characterization of MtoD from *Sideroxydans lithotrophicus*: a cytochrome c electron shuttle used in lithoautotrophic growth. *Front. Microbiol.* **6**, 332 (2015).
182. Bird, L. J., Bonnefoy, V. & Newman, D. K. Bioenergetic challenges of microbial iron metabolisms. *Trends Microbiol.* **19**, 330–340 (2011).
183. Field, S. J. et al. Purification and magneto-optical spectroscopic characterization of cytoplasmic membrane and outer membrane multiheme c-type cytochromes from *Shewanella frigidimarina* NCIMB400. *J. Biol. Chem.* **275**, 8515–8522 (2000).
184. Giffaut, E. et al. Andra thermodynamic database for performance assessment: ThermoChimie. *Appl. Geochem.* **49**, 225–236 (2014).
185. Salmon, T. P., Rose, A. L., Neilan, B. A. & Waite, T. D. The FeL model of iron acquisition: nondissociative reduction of ferric complexes in the marine environment. *Limnol. Oceanogr.* **51**, 1744–1754 (2006).
186. Navrotsky, A., Mazeina, L. & Majzlan, J. Size-driven structural and thermodynamic complexity in iron oxides. *Science* **319**, 1635–1638 (2008).
187. Gorski, C. A., Edwards, R., Sander, M., Hofstetter, T. B. & Stewart, S. M. Thermodynamic characterization of iron oxide–aqueous Fe^{2+} redox couples. *Environ. Sci. Technol.* **50**, 8538–8547 (2016). **One of the first examples of using electrochemical methods to better understand the range of redox potentials present in different iron phases**.
188. Robie, R. A. & Heminway, B. S. Thermodynamic properties of minerals and related substances at 298.15 K and 1 bar (105 pascals) pressure and at higher temperatures. (United States Printing Office, 1995).
189. Navrotsky, A., Ma, C., Lilova, K. & Birkner, N. Nanophase transition metal oxides show large thermodynamically driven shifts in oxidation-reduction equilibria. *Science* **330**, 199–201 (2010).
190. Robie, R. A. & Bethke, P. *Molar Volumes and Densities of Minerals*. Report TEI-822 (United States Department of the Interior Geological Survey, 1962).
191. Gorski, C. A., Nurmi, J. T., Tratnyek, P. G., Hofstetter, T. B. & Scherer, M. M. Redox behavior of magnetite: implications for contaminant reduction. *Environ. Sci. Technol.* **44**, 55–60 (2010).
192. Gorski, C. A., Klüpfel, L. E., Voegelin, A., Sander, M. & Hofstetter, T. B. Redox properties of structural Fe in clay minerals: 3. Relationships between smectite redox and structural properties. *Environ. Sci. Technol.* **47**, 13477–13485 (2013).
193. Oswald, K. et al. Aerobic gammaproteobacterial methanotrophs mitigate methane emissions from oxic and anoxic lake waters. *Limnol. Oceanogr.* **61**, S101–S118 (2016).
194. Braunschweig, J., Bosch, J. & Meckenstock, R. U. Iron oxide nanoparticles in geomicrobiology: from biogeochemistry to bioremediation. *N. Biotechnol.* **30**, 793–802 (2013).
195. Villa, R. D., Trovó, A. G. & Nogueira, R. F. P. Environmental implications of soil remediation using the Fenton process. *Chemosphere* **71**, 43–50 (2008).
196. Wagai, R. & Mayer, L. M. Sorptive stabilization of organic matter in soils by hydrous iron oxides. *Geochim. Cosmochim. Acta* **71**, 25–35 (2007).
197. Nitzsche, K. S. et al. Arsenic removal from drinking water by a household sand filter in Vietnam — effect of filter usage practices on arsenic removal efficiency and microbiological water quality. *Sci. Total. Environ.* **502**, 526–536 (2015).
198. Sipos, P., Németh, T., Kis, V. K. & Mohai, I. Sorption of copper, zinc and lead on soil mineral phases. *Chemosphere* **73**, 461–469 (2008).

199. Poulton, S. W. & Canfield, D. E. Development of a sequential extraction procedure for iron: implications for iron partitioning in continentally derived particulates. *Chem. Geol.* **214**, 209–221 (2005).
200. Schaedler, F., Kappler, A. & Schmidt, C. A revised iron extraction protocol for environmental samples rich in nitrite and carbonate. *Geomicrobiol. J.* **35**, 23–30 (2018).
201. Porsch, K. & Kappler, A. Fe^{II} oxidation by molecular O_2 during HCl extraction. *Environ. Chem.* **8**, 190–197 (2011).
202. Roden, E. E. & Zachara, J. M. Microbial reduction of crystalline iron(III) oxides: Influence of oxide surface area and potential for cell growth. *Environ. Sci. Technol.* **30**, 1618–1628 (1996).
203. Tessier, A., Campbell, P. G. C. & Bisson, M. Sequential extraction procedure for the speciation of particulate trace metals. *Anal. Chem.* **51**, 844–851 (1979).
204. Stookey, L. L. Ferrozine - a new spectrophotometric reagent for iron. *Anal. Chem.* **42**, 779–781 (1970).
205. Clark, L. J. Iron(II) determination in the presence of iron(III) using 4,7-diphenyl-1,10-phenanthroline. *Anal. Chem.* **34**, 348–352 (1962).
206. Viollier, E., Inglett, P. W., Hunter, K., Roychoudhury, A. N. & Van Cappellen, P. The ferrozine method revisited: Fe(II)/Fe(III) determination in natural waters. *Appl. Geochem.* **15**, 785–790 (2000).

Acknowledgements
The authors acknowledge funding for several research grants from the German Research Foundation (DFG), in particular the Collaborative Research Center CAMPOS (DFG grant agreement SFB 1253/1) and the priority programme EarthShape.

Author contributions
A.K. and C.B. initiated the manuscript, designed the content, wrote the manuscript, created some of the figures, and compiled and revised all content. E.D.S., M.M., U.L. and J.M.B. wrote the manuscript and created some of the figures.

Competing interests
The authors declare no competing interests.

Peer review information
Nature Reviews Microbiology thanks J. Gralnick, who co-reviewed with A. Jain, J. Senko and the other, anonymous, reviewer(s) for their contribution to the peer review of this work.

Publisher's note
Springer Nature remains neutral with regard to jurisdictional claims in published maps and institutional affiliations.